



Stony Brook
University



Diamond is a Beam's Best Friend

John Smedley
Brookhaven National Laboratory

Diamond x-ray sensors
Transparent x-ray camera
Sensors for radiation therapy

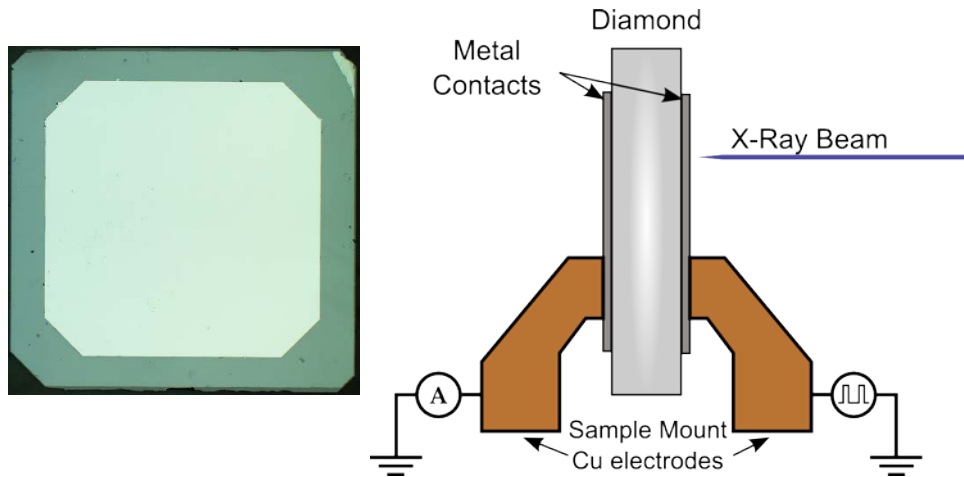
Diamond as an X-ray Sensor

Diamond Advantages:

- Low X-ray Absorption
- High Thermal Conductivity
- Mechanical Strength
- Radiation Hardness
- Indirect bandgap

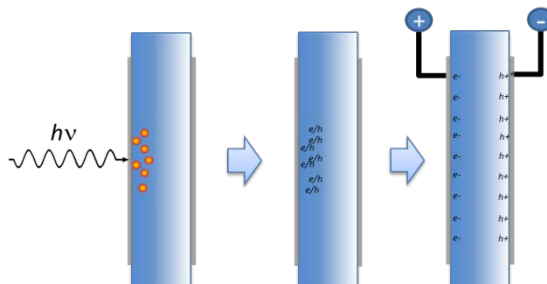
Sample Information:

- Electrical grade CVD single crystal diamond
- (100) surface orientation
- ~1 ppb nitrogen impurity
- Typical size: 4mm x 4mm x 50 μm



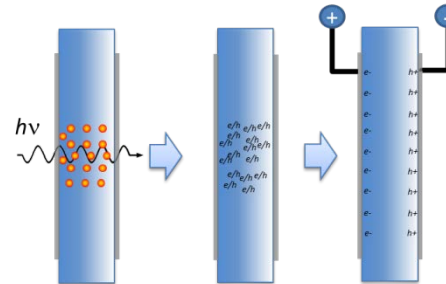
X-ray generated charge carriers

Low energy x-ray



Electron hole pairs created near incident electrode: must move entire thickness of the diamond

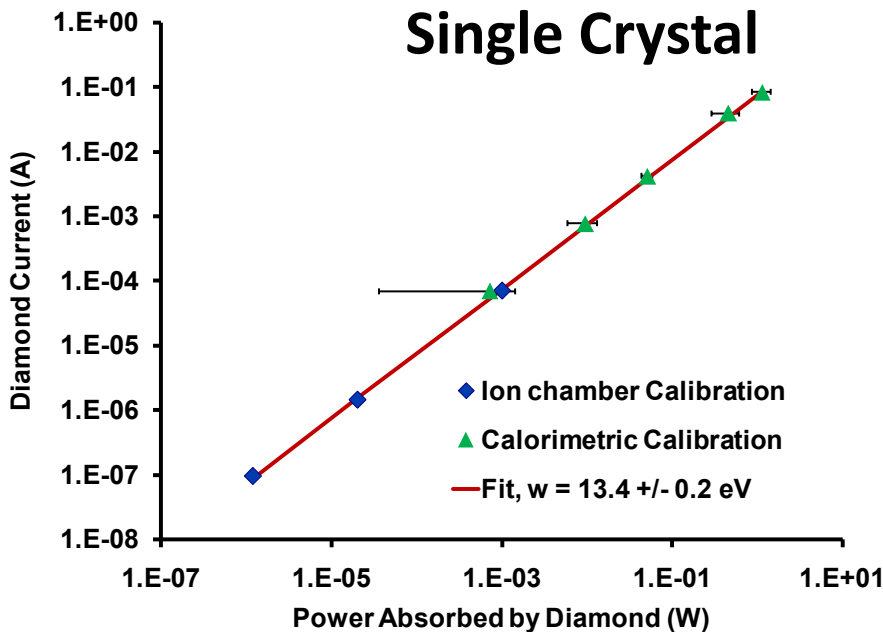
High energy x-ray



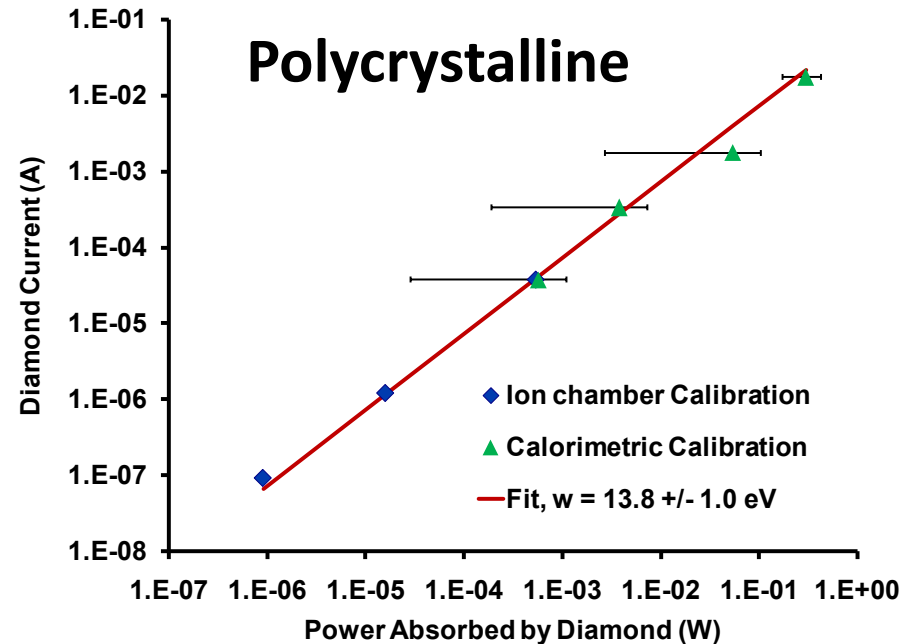
Electron hole pairs created throughout the thickness creating a column of electron-hole pairs

Response vs Flux and Bias

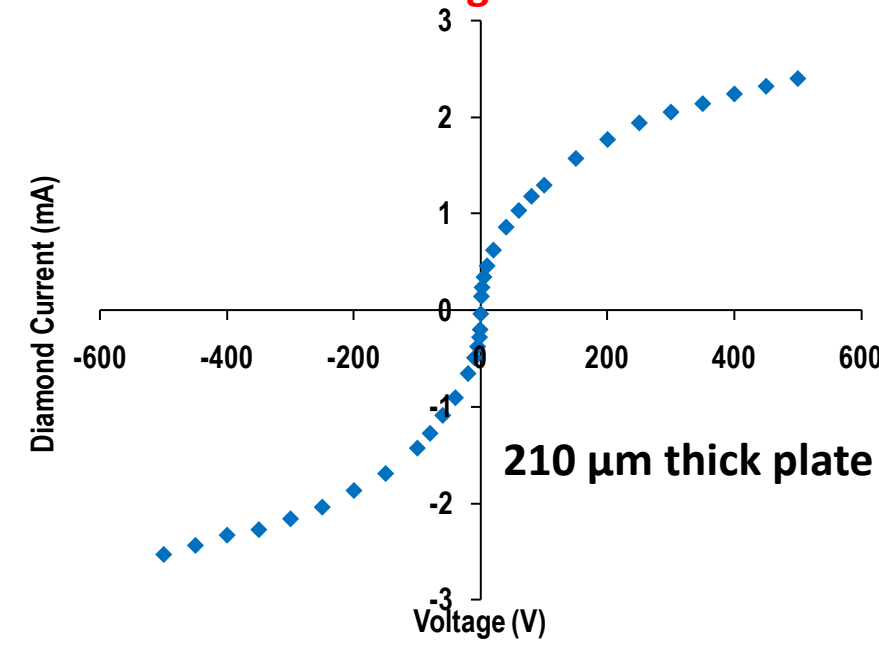
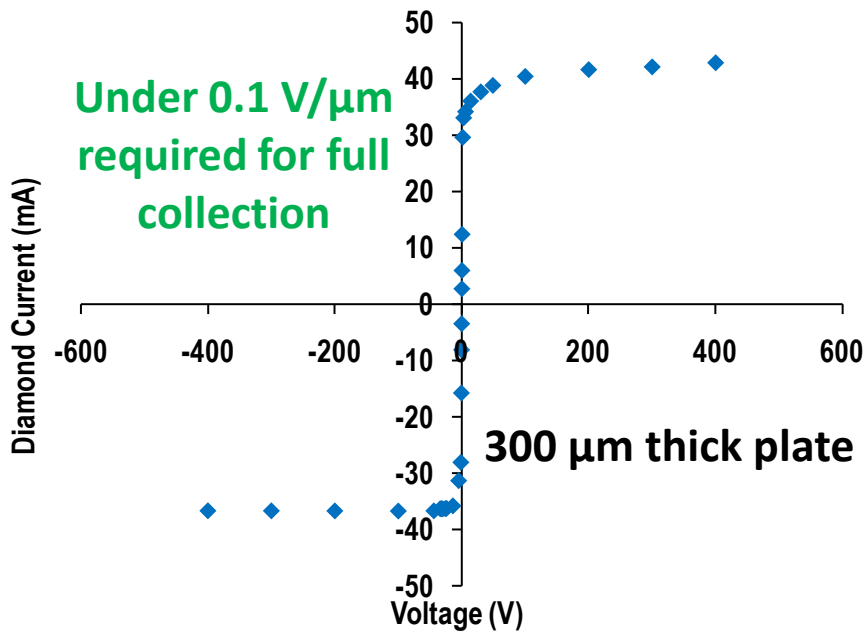
Single Crystal



Polycrystalline



Response to incident flux linear over 11 orders of magnitude



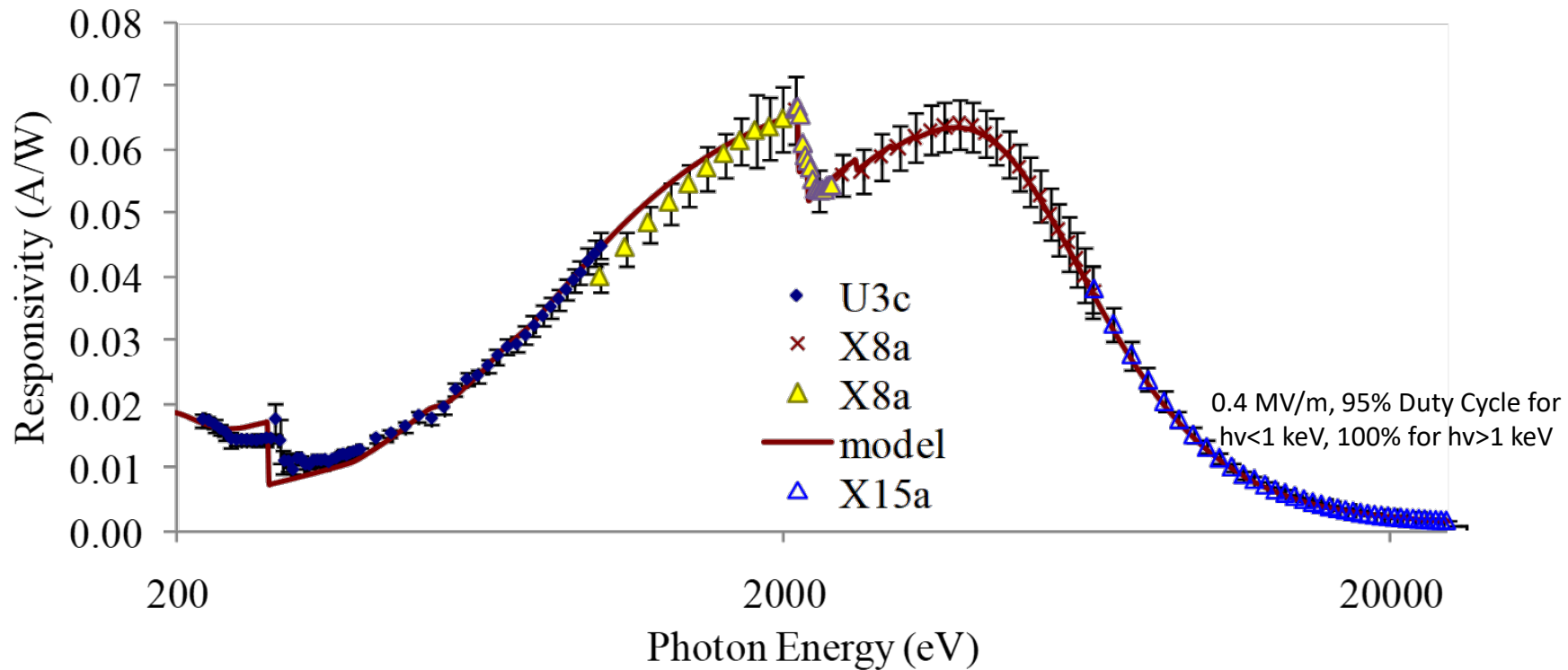
Under $0.1 \text{ V}/\mu\text{m}$
required for full
collection

$300 \mu\text{m}$ thick plate

$210 \mu\text{m}$ thick plate

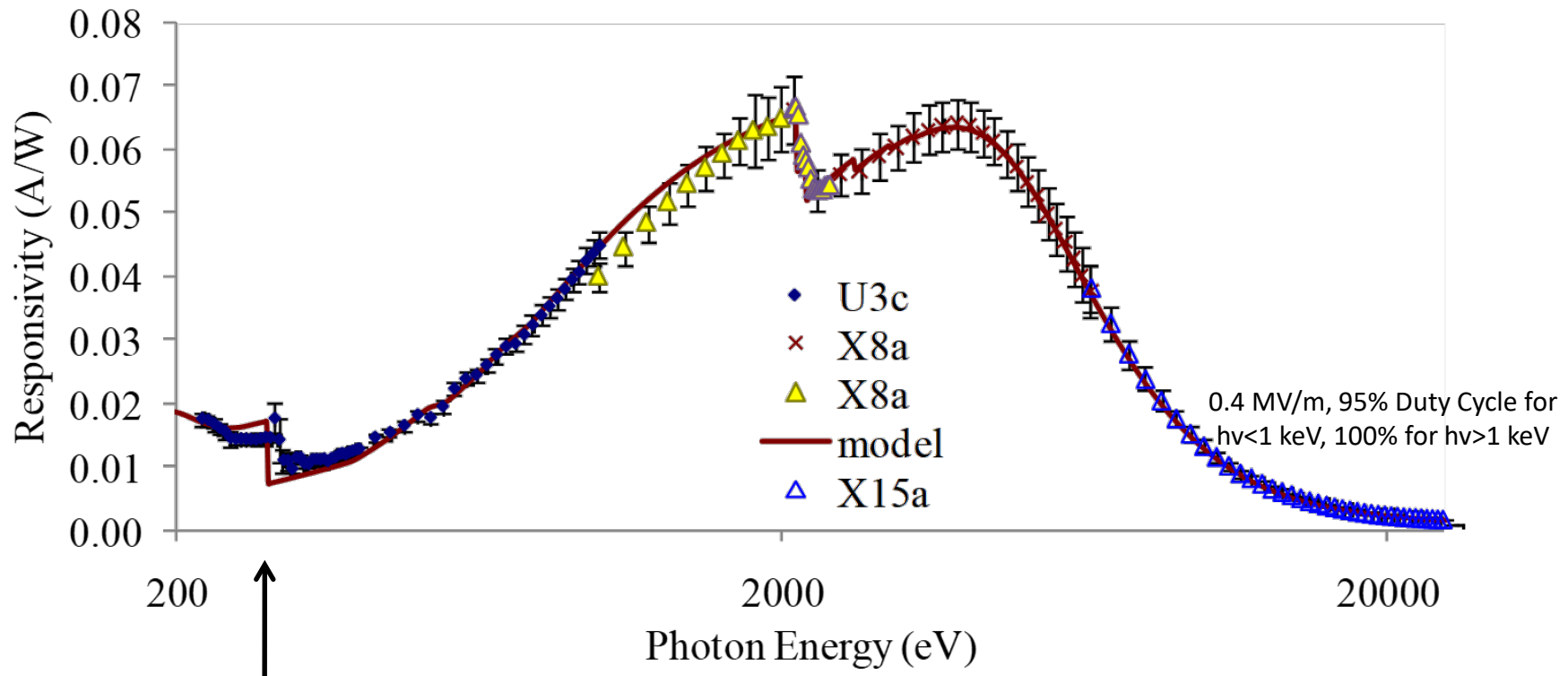
Responsivity vs Photon Energy

$$S = \frac{1}{w} e^{-t_{metal}/\lambda_{metal}} \left(1 - e^{-t_{dia}/\lambda_{dia}}\right) CE[v, F]$$



Responsivity vs Photon Energy

$$S = \frac{1}{w} e^{-t_{metal}/\lambda_{metal}} \left(1 - e^{-t_{dia}/\lambda_{dia}}\right) CE[v, F]$$

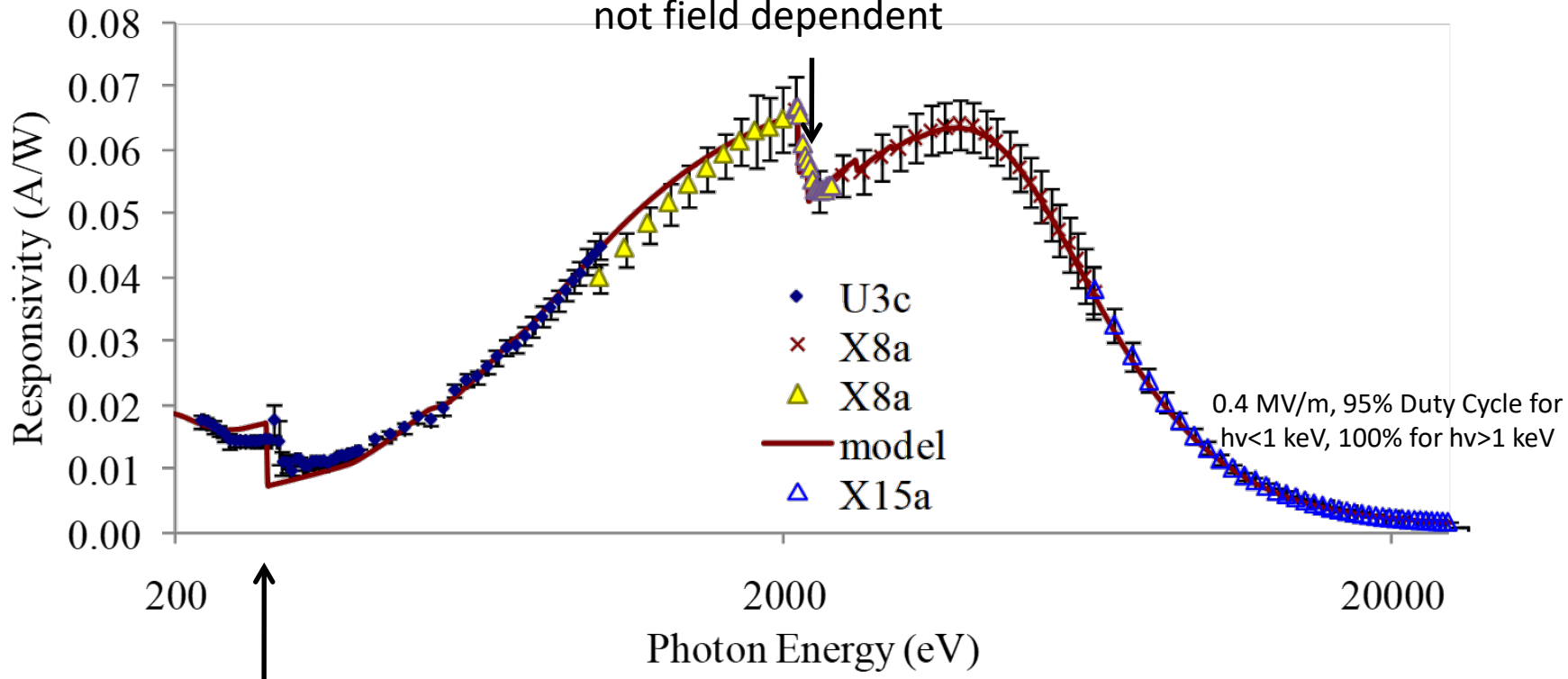


C K edge feature is field dependent, caused by incomplete carrier collection
for carriers produced near incident electrode – electrons diffuse into incident contact
and are lost

Responsivity vs Photon Energy

$$S = \frac{1}{w} e^{-t_{metal}/\lambda_{metal}} \left(1 - e^{-t_{dia}/\lambda_{dia}}\right) CE[v, F]$$

Platinum M edge feature due to loss of photons absorbed by incident contact
not field dependent

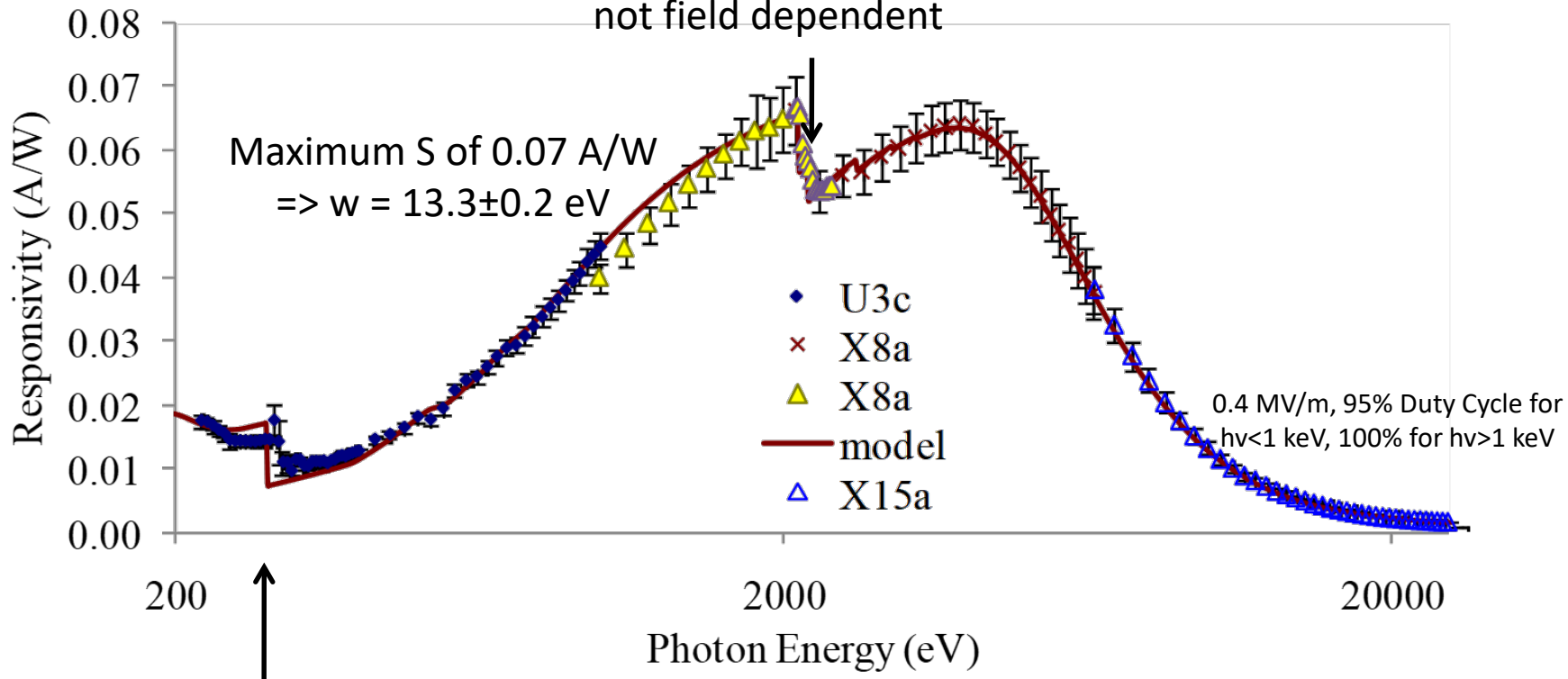


C K edge feature is field dependent, caused by incomplete carrier collection
for carriers produced near incident electrode – electrons diffuse into incident contact
and are lost

Responsivity vs Photon Energy

$$S = \frac{1}{w} e^{-t_{metal}/\lambda_{metal}} \left(1 - e^{-t_{dia}/\lambda_{dia}}\right) CE[v, F]$$

Platinum M edge feature due to loss of photons absorbed by incident contact
not field dependent

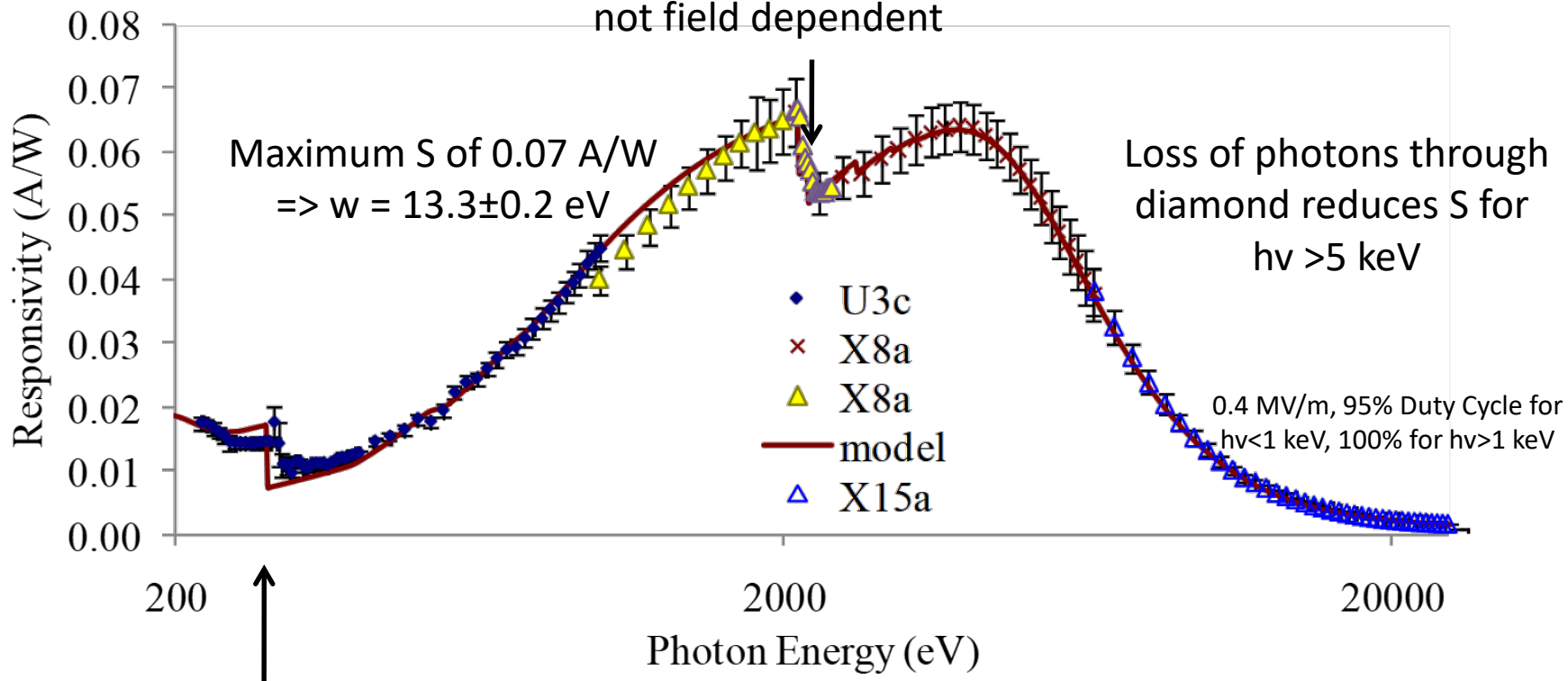


C K edge feature is field dependent, caused by incomplete carrier collection
for carriers produced near incident electrode – electrons diffuse into incident contact
and are lost

Responsivity vs Photon Energy

$$S = \frac{1}{w} e^{-t_{metal}/\lambda_{metal}} \left(1 - e^{-t_{dia}/\lambda_{dia}}\right) CE[v, F]$$

Platinum M edge feature due to loss of photons absorbed by incident contact
not field dependent

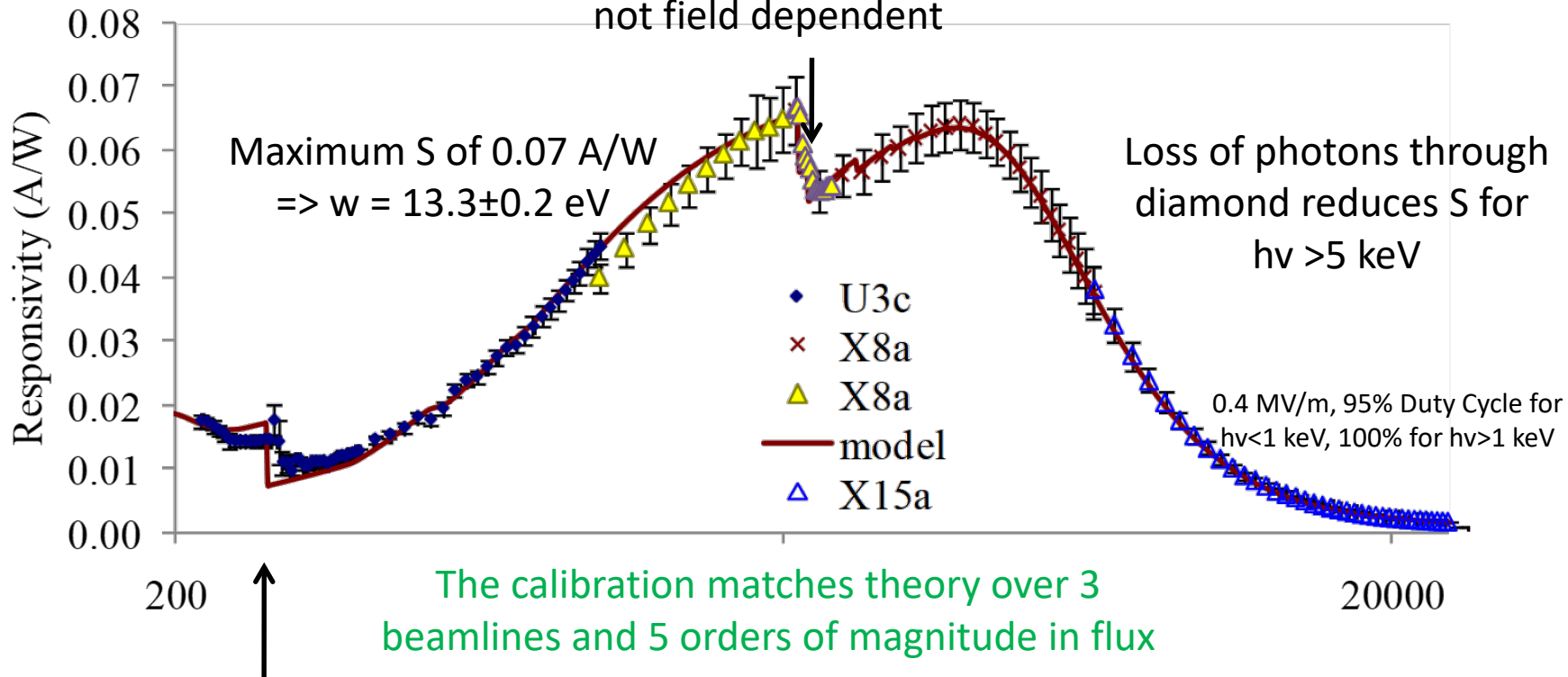


C K edge feature is field dependent, caused by incomplete carrier collection
for carriers produced near incident electrode – electrons diffuse into incident contact
and are lost

Responsivity vs Photon Energy

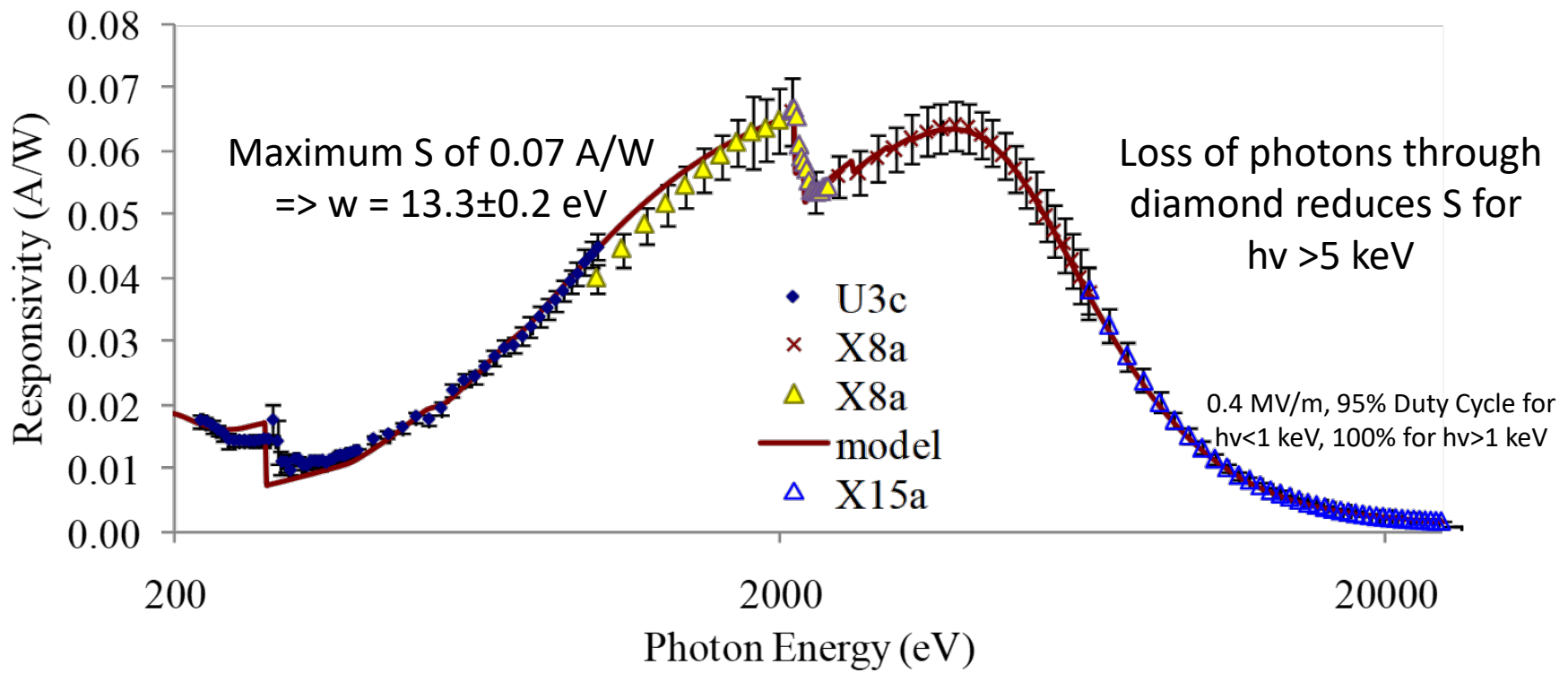
$$S = \frac{1}{w} e^{-t_{metal}/\lambda_{metal}} \left(1 - e^{-t_{dia}/\lambda_{dia}}\right) CE[v, F]$$

Platinum M edge feature due to loss of photons absorbed by incident contact
not field dependent



C K edge feature is field dependent, caused by incomplete carrier collection
for carriers produced near incident electrode – electrons diffuse into incident contact
and are lost

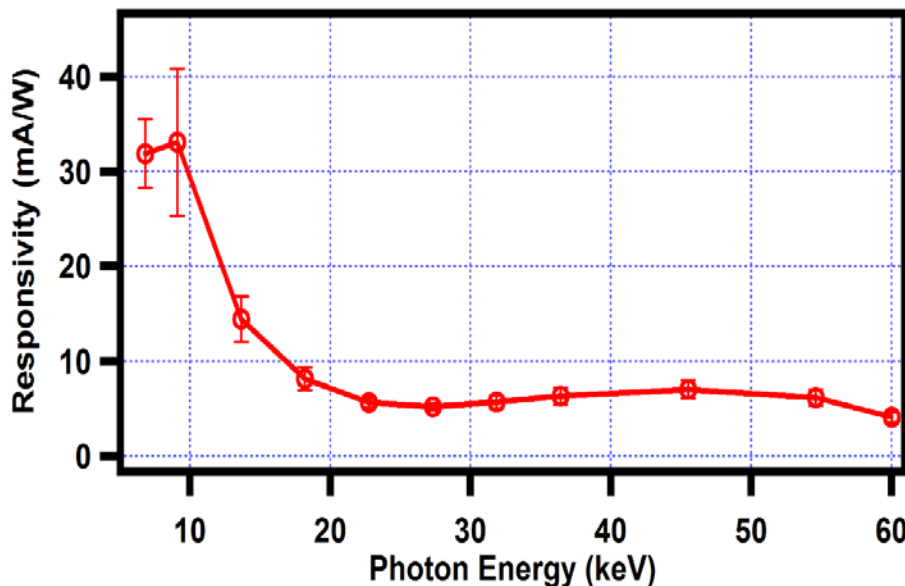
Kinda Useless at High Energy, Right?



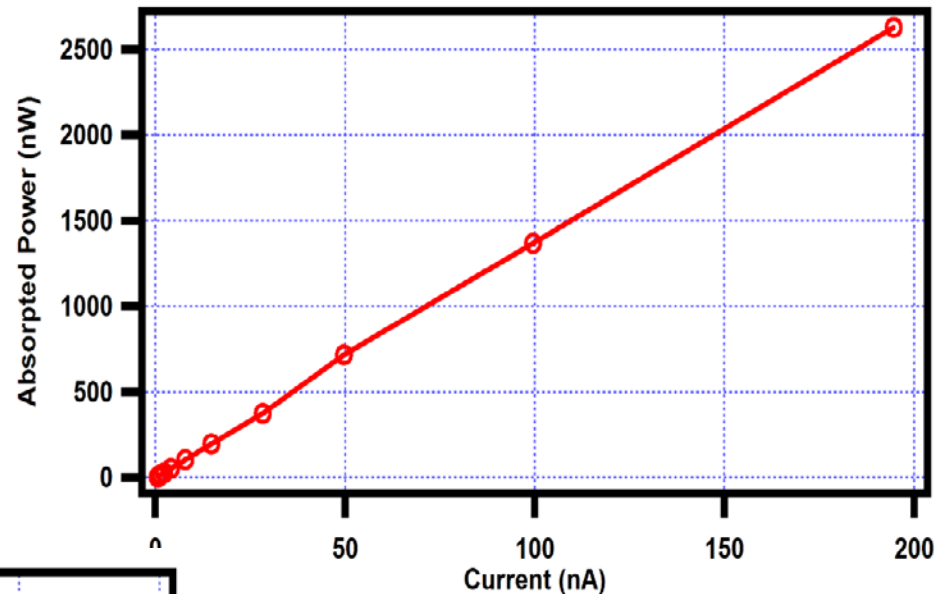
Compton Regime

Actually, above 20 keV, cross section is Compton dominated for carbon

Responsivity stabilizes (and actually rises). Compton cross section is independent of Z (though the onset of Compton dominated regime is Z dependent)



Diamond responsivity data between 6.8-60 keV @A2



Linearity at XPD at NSLS-II (67 keV)

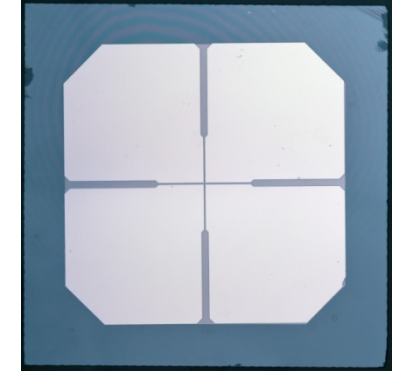
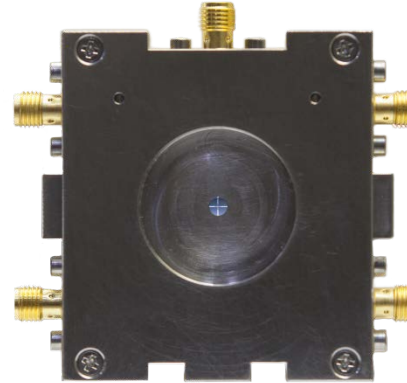
Beam monitoring (pulse to pulse variation) should be possible

Also, a “Compton spectrometer” may be possible – tagging a photon in diamond and on a second detector. Measuring energy deposited in diamond and angle is sufficient to know photon energy.

Diamond Beam Position Monitors

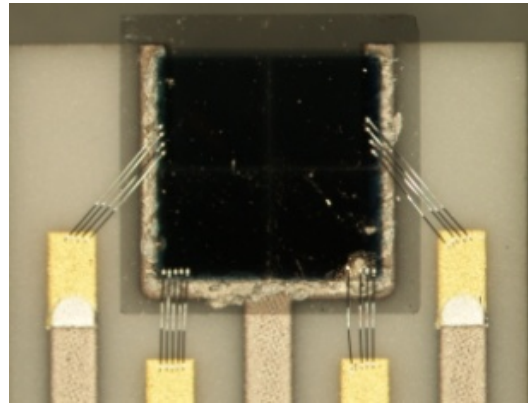
Circuit Board Mounted

Pt metallization
wire-bonded electrodes
SMA/LEMO connectors



Application specific –
X-Ray fluorescence,
microEXAFS

Ag diamond metallization
Ceramic board
Single channel detector designed
for use with polycapillary



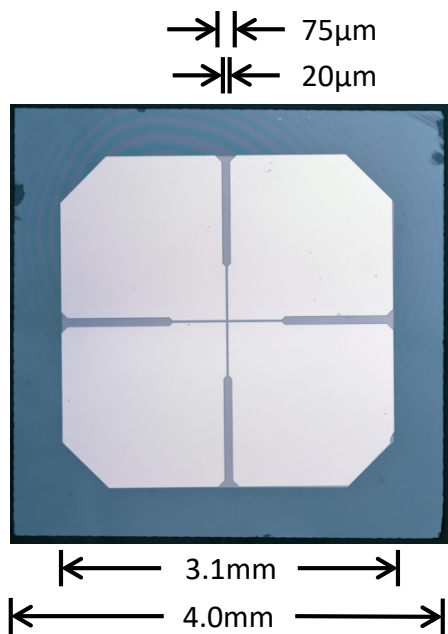
White BPM (X25)

Mini-gap undulator
~100W incident power
Large beam



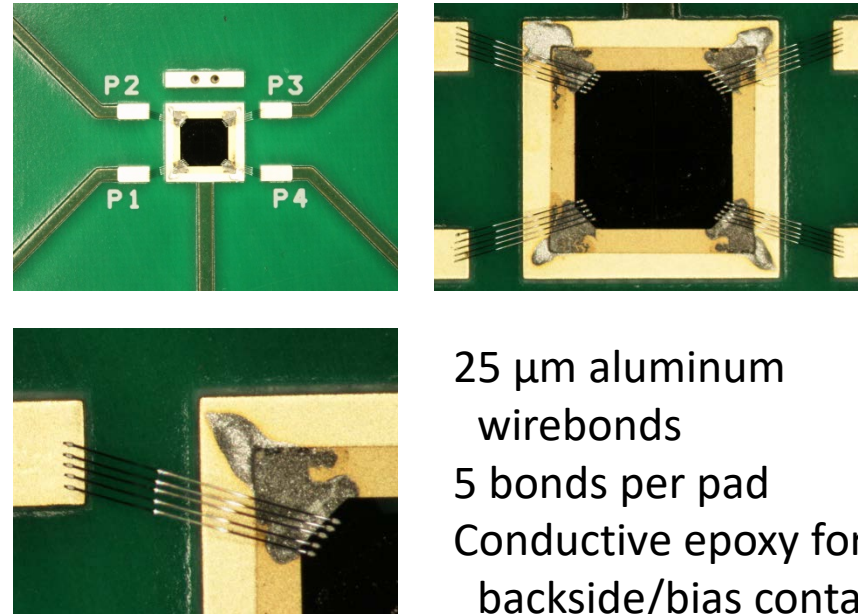
Fabrication

Lithography @ CFN

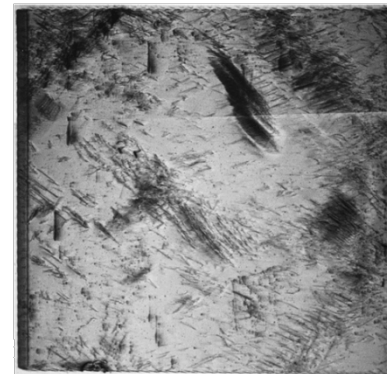


Electronic grade single crystal
(100) diamond
30-50 μm thick
20 μm street over a 1mm
center region
Metallization: 25 nm Pt

Wire Bonding - Instrumentation



Topography – NSLS/CHESS

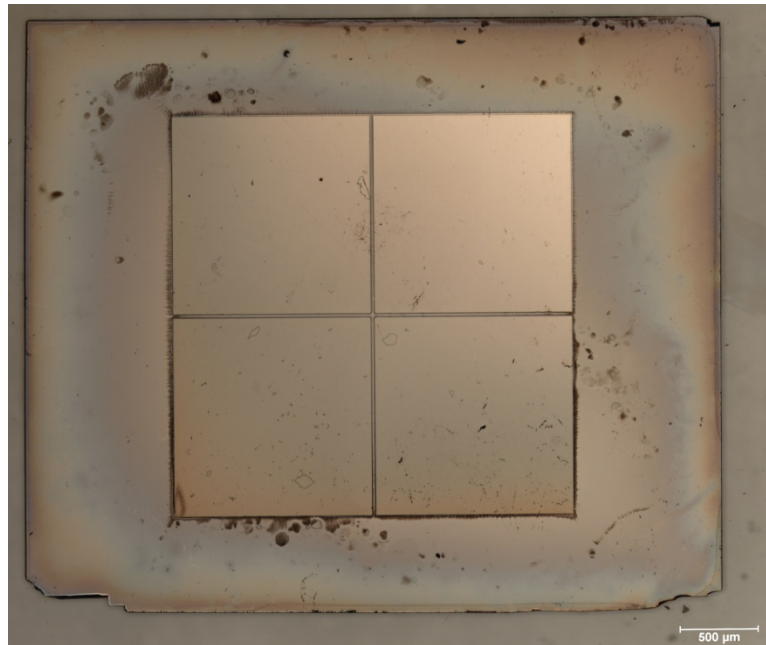


White beam topography
Prior to slicing

New Fabrication Tools

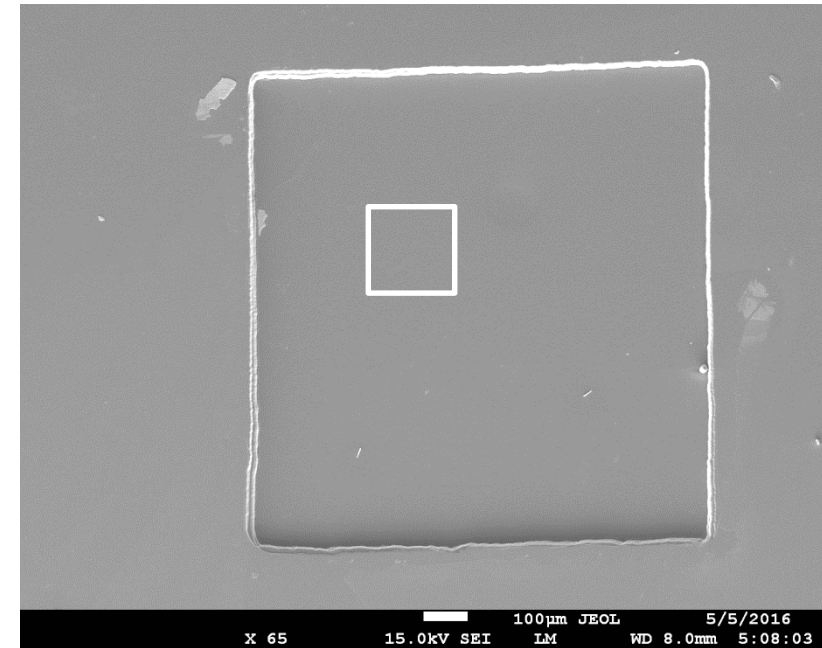
Patterned UNCD Contacts

- Diamond Contacts – no longer the weakest link
- No fluorescent lines



RIE ultrathin layers

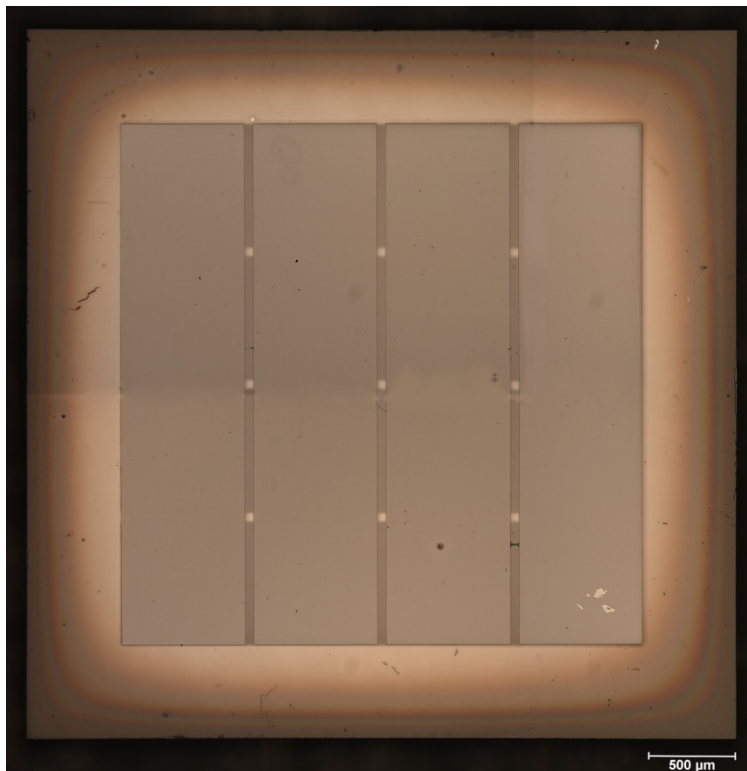
- 4 μm membranes
- Transmits 2 keV photons
- Potentially much faster response
- 4 devices in use at SMI



New Fabrication Tools

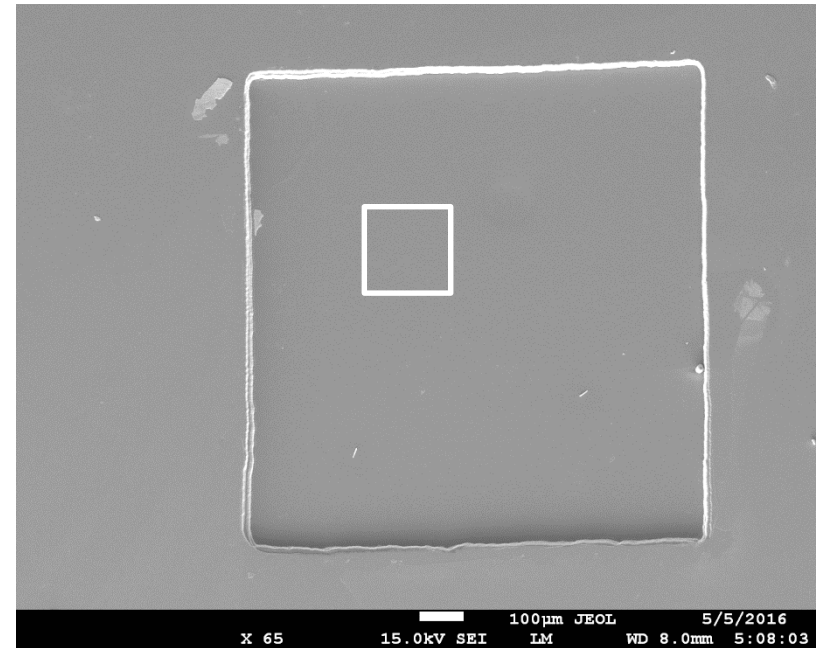
Patterned UNCD Contacts

- Diamond Contacts – no longer the weakest link
- No fluorescent lines



RIE ultrathin layers

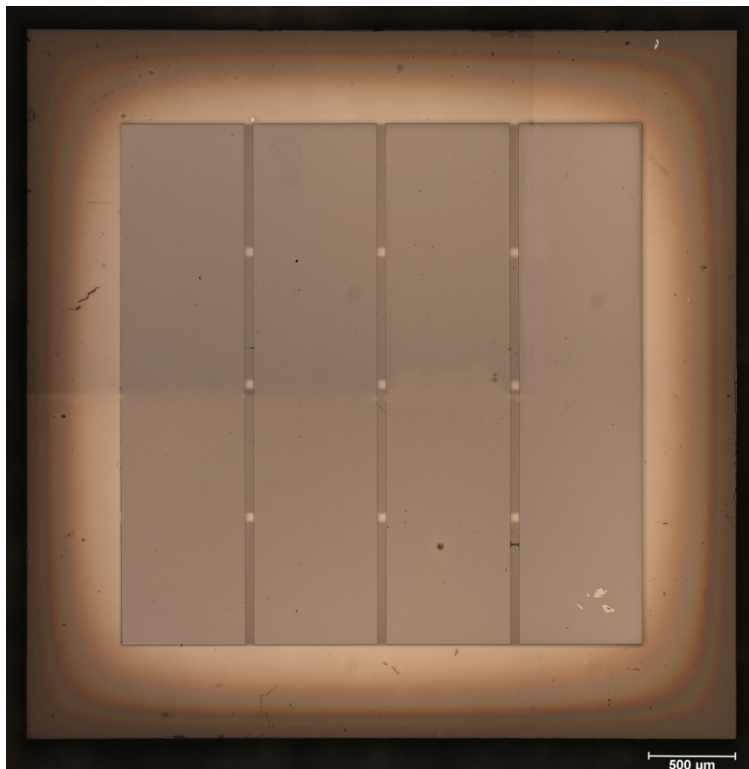
- 4 μm membranes
- Transmits 2 keV photons
- Potentially much faster response
- 4 devices in use at SMI



New Fabrication Tools

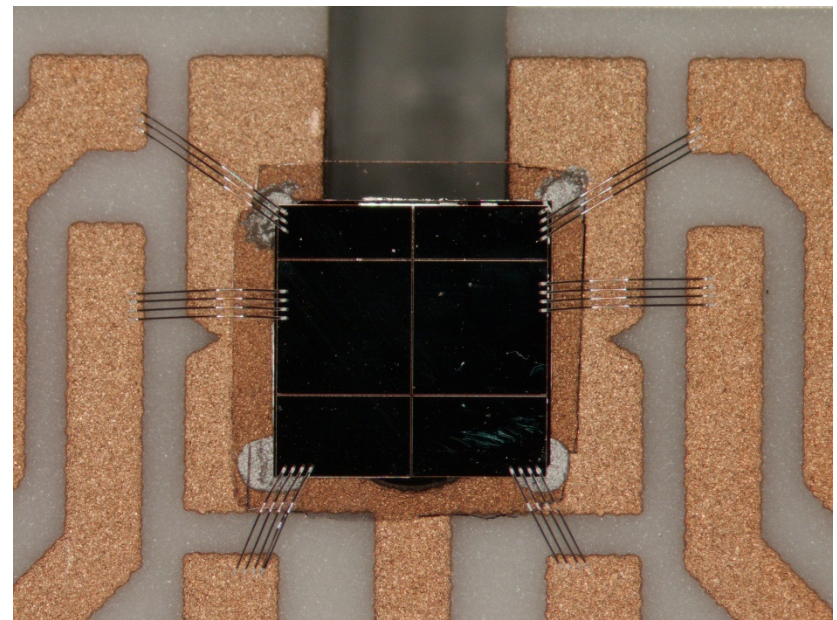
Patterned UNCD Contacts

- Diamond Contacts – no longer the weakest link
- No fluorescent lines



RIE ultrathin layers

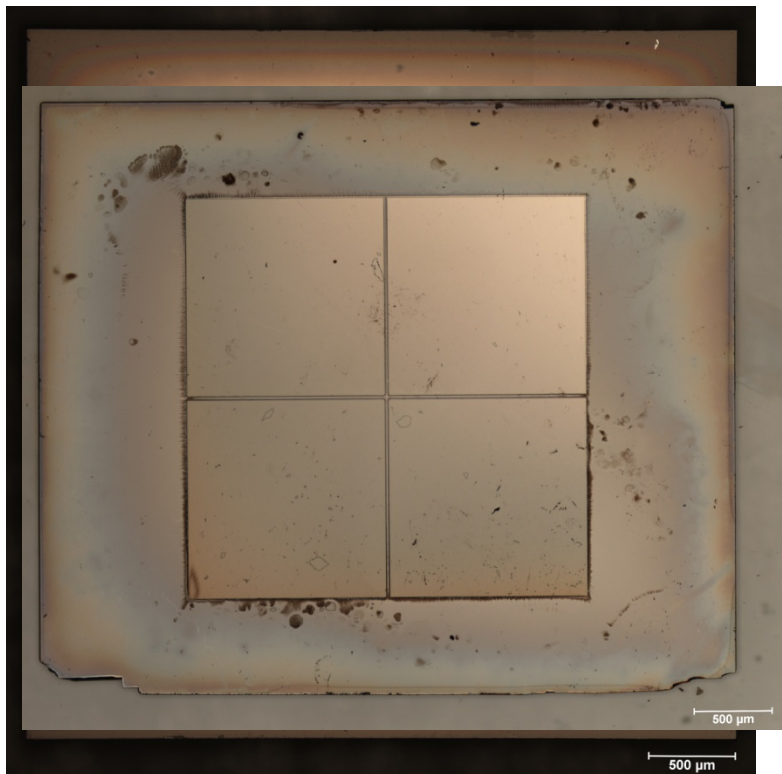
- 4 μm membranes
- Transmits 2 keV photons
- Potentially much faster response
- 4 devices in use at SMI



New Fabrication Tools

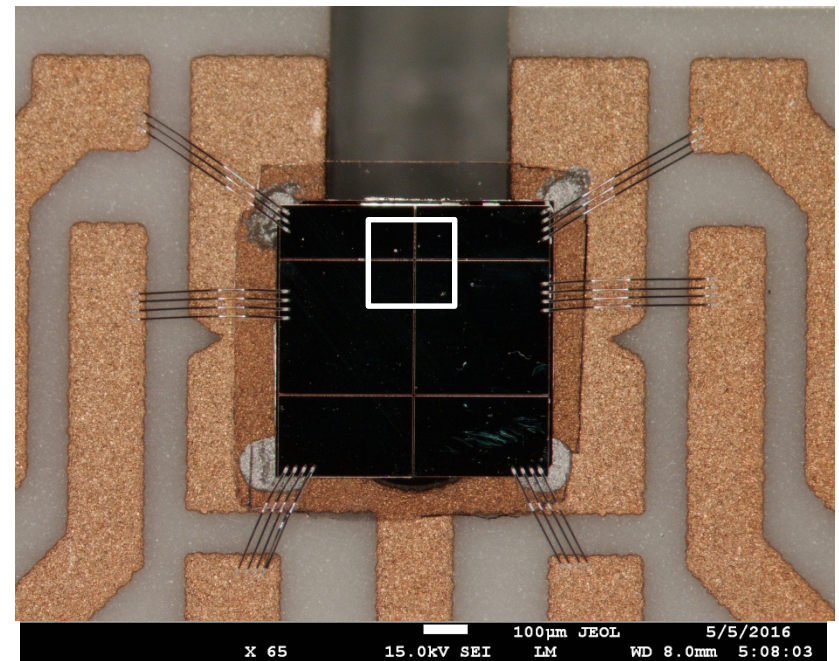
Patterned UNCD Contacts

- Diamond Contacts – no longer the weakest link
- No fluorescent lines

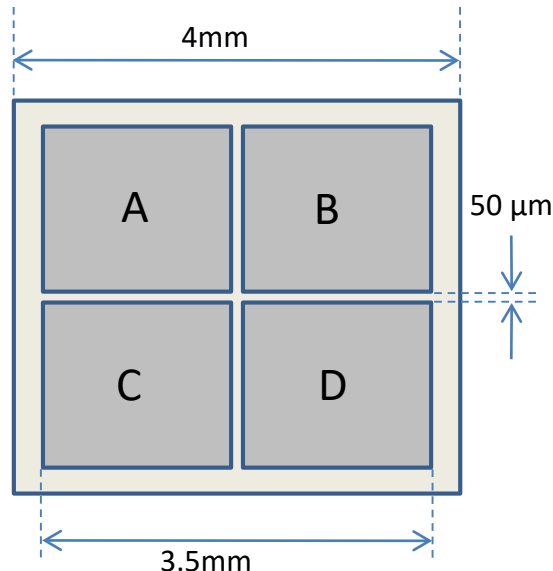


RIE ultrathin layers

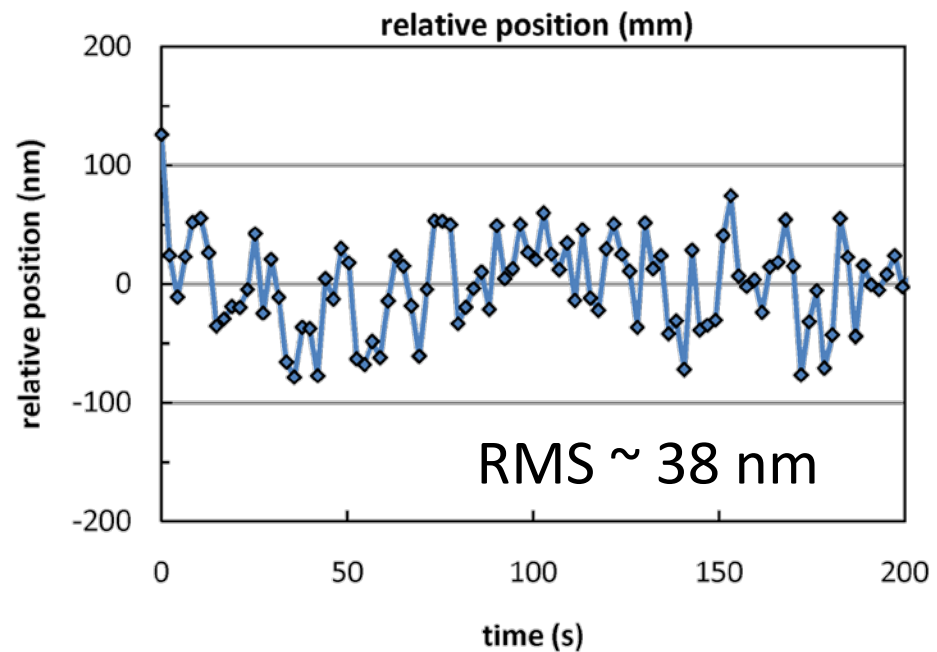
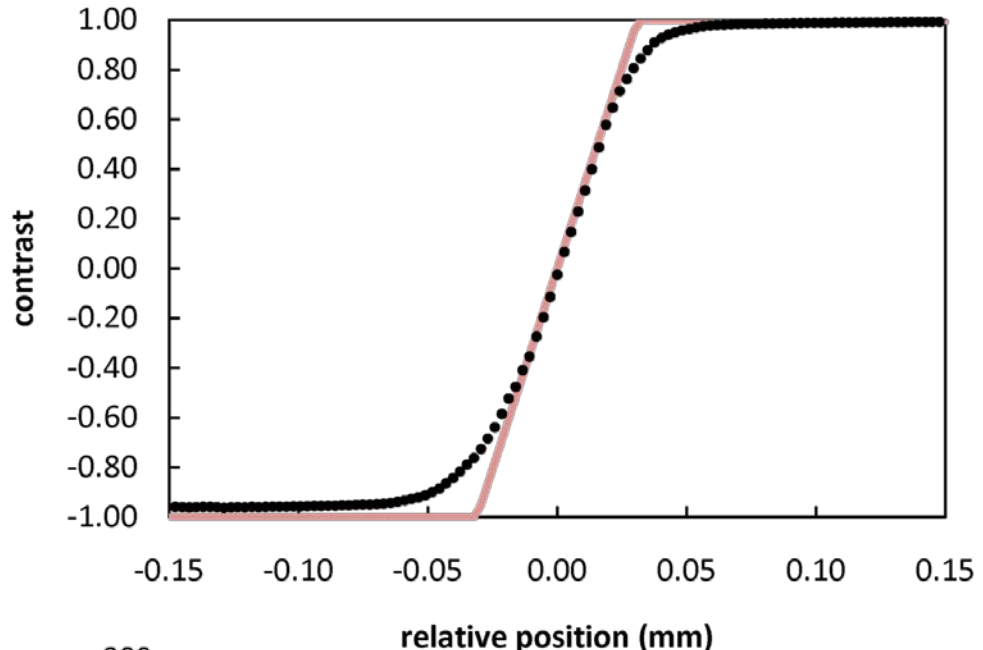
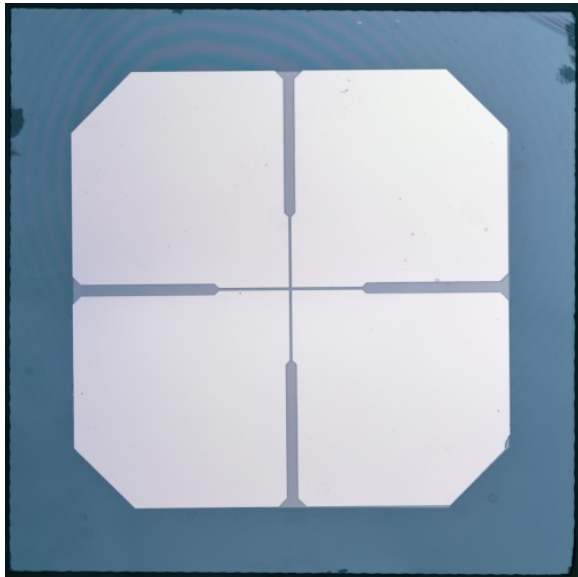
- 4 μm membranes
- Transmits 2 keV photons
- Potentially much faster response
- 4 devices in use at SMI



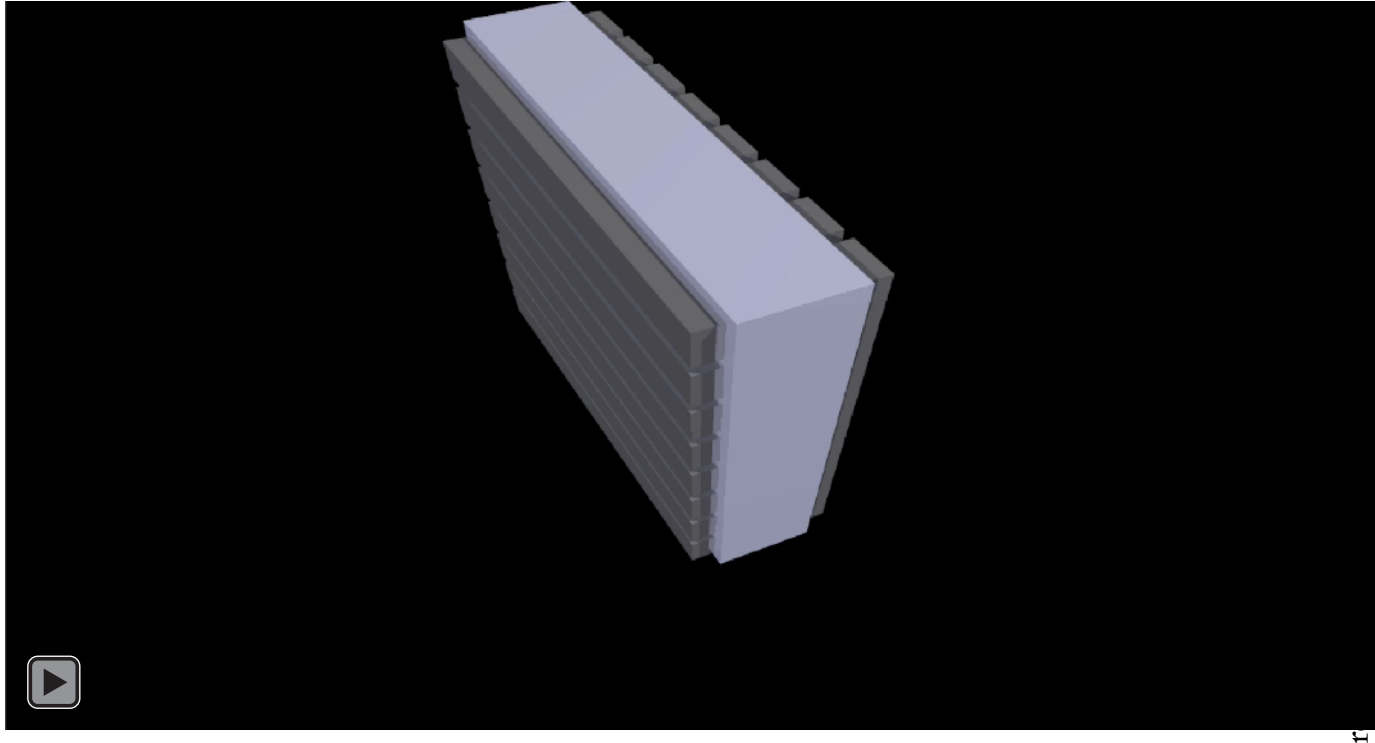
Beam Position Monitors



$$X = G_x \frac{(I_B + I_D) - (I_A + I_C)}{I_A + I_B + I_C + I_D}$$



Pixelated Diamond Window



Pixels are created by metalizing one side of the diamond with horizontal stripes and the other with vertical stripes. As the x-rays pass through the diamond, the induced current is collected in each vertical stripe, while the bias is applied to individual stripes on the other side. This bias is cycled, allowing readout of one line of “pixels” at a time.

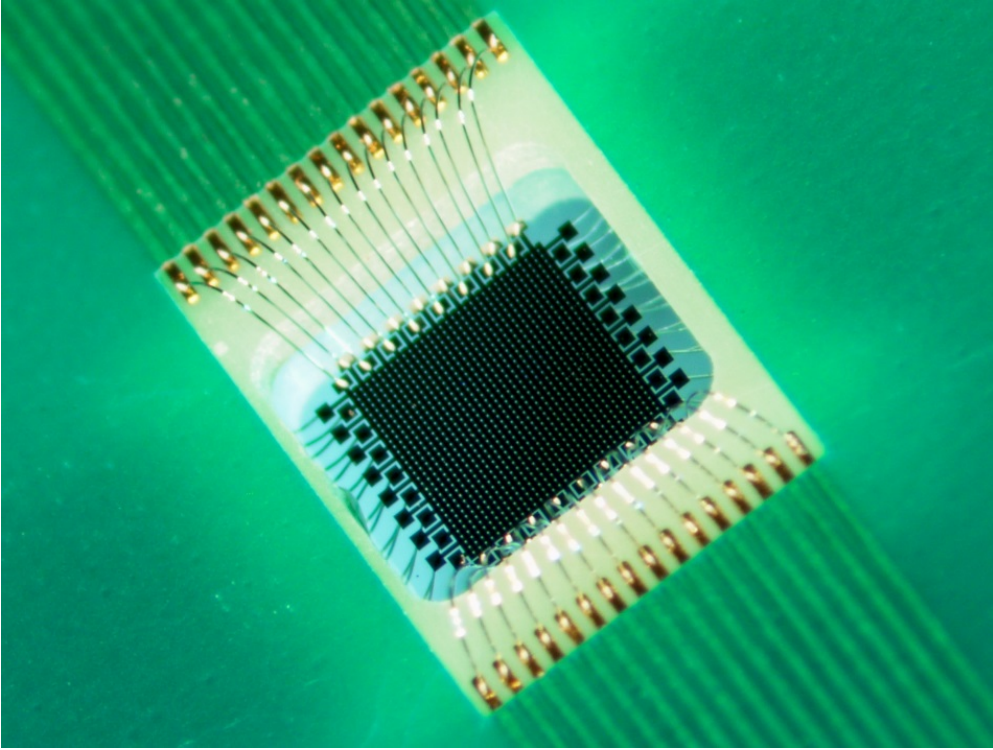
Image Readout

- 32 x 32 stripes, yielding 1024 pixels
- Only one row is active at a time minimizing ohmic heat generation.
- Project goal of real time imaging at 1 Hz, currently at 32 Hz
- Up to \sim 10mA per pixel
- **FPGA controlled, versatile operating modes**

Window Fabrication

- The diamond sensor will be brazed to a stainless steel vacuum flange.
- The diamond and electronic interconnects will be protected by a metal mask.
- Heat dissipation provided by water cooling.

Pixelated Diamond Window



Pixels are created by metalizing one side of the diamond with horizontal stripes and the other with vertical stripes. As the x-rays pass through the diamond, the induced current is collected in each vertical stripe, while the bias is applied to individual stripes on the other side. This bias is cycled, allowing readout of one line of “pixels” at a time.

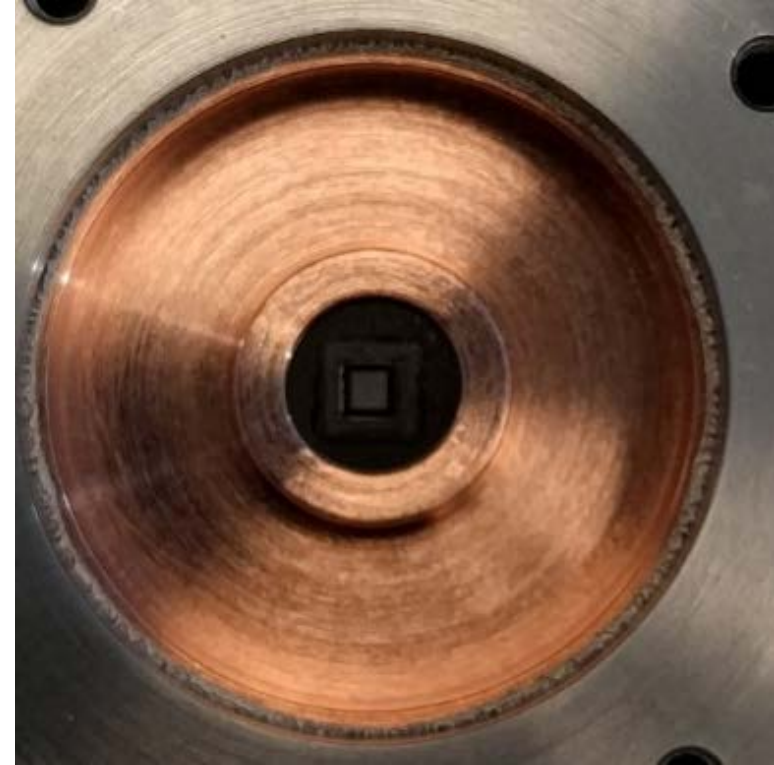
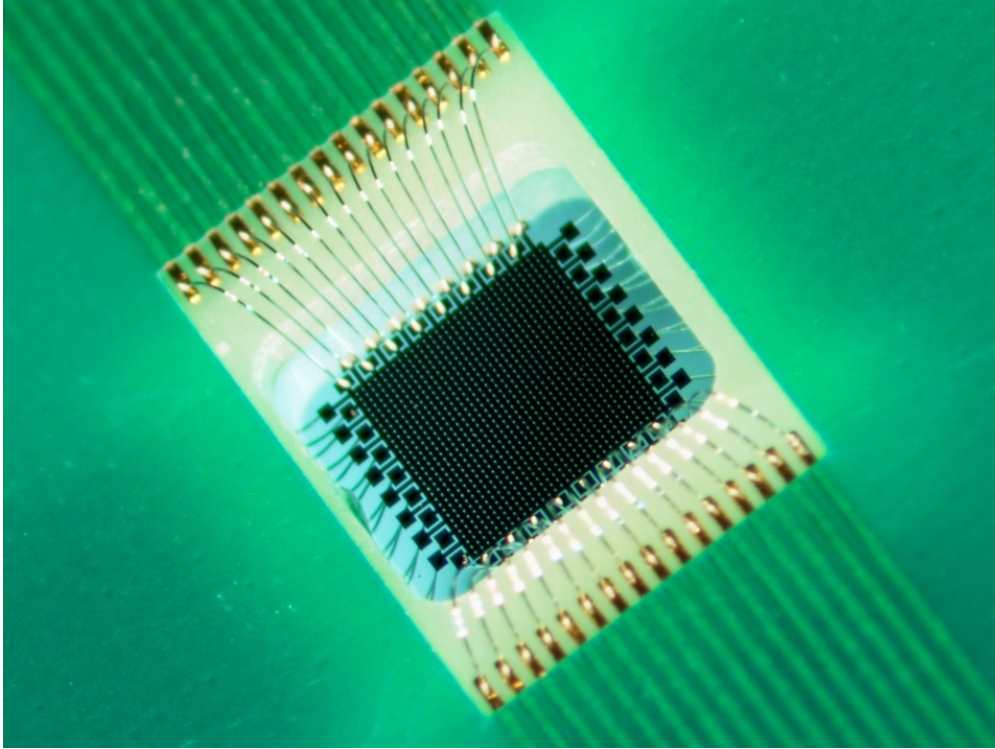
Image Readout

- 32 x 32 stripes, yielding 1024 pixels
- Only one row is active at a time minimizing ohmic heat generation.
- Project goal of real time imaging at 1 Hz, currently at 32 Hz
- Up to \sim 10mA per pixel
- **FPGA controlled, versatile operating modes**

Window Fabrication

- The diamond sensor brazed to a stainless steel vacuum flange.
- The diamond and electronic interconnects will be protected by a metal mask.
- Heat dissipation provided by water cooling.

Pixelated Diamond Window



Pixels are created by metalizing one side of the diamond with horizontal stripes and the other with vertical stripes. As the x-rays pass through the diamond, the induced current is collected in each vertical stripe, while the bias is applied to individual stripes on the other side. This bias is cycled, allowing readout of one line of “pixels” at a time.

Image Readout

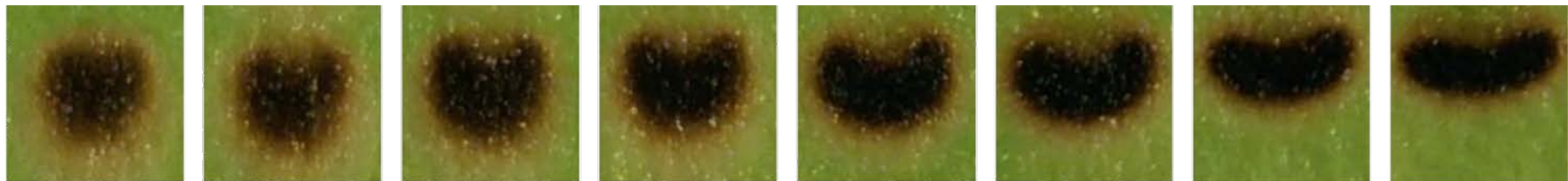
- 32 x 32 stripes, yielding 1024 pixels
- Only one row is active at a time minimizing ohmic heat generation.
- Project goal of real time imaging at 1 Hz, currently at 32 Hz
- Up to \sim 10mA per pixel
- **FPGA controlled, versatile operating modes**

Window Fabrication

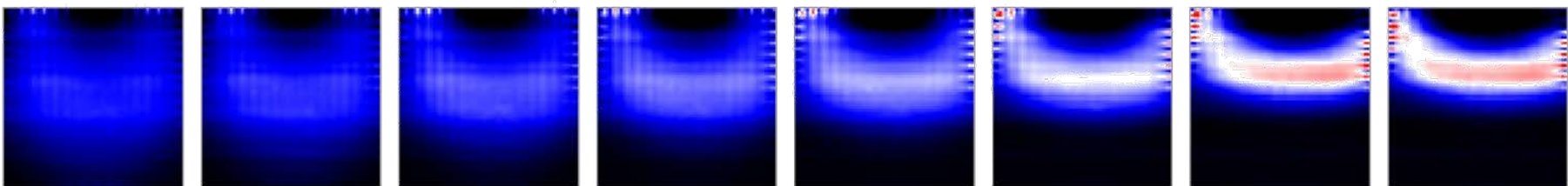
- The diamond sensor brazed to a stainless steel vacuum flange.
- The diamond and electronic interconnects will be protected by a metal mask.
- Heat dissipation provided by water cooling.

Beam Imaging

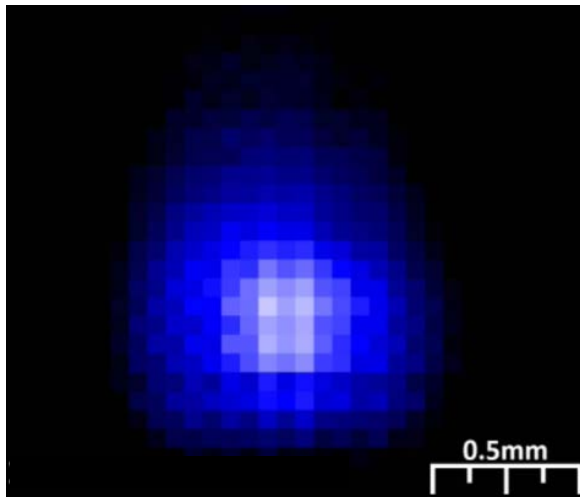
X-ray Burn



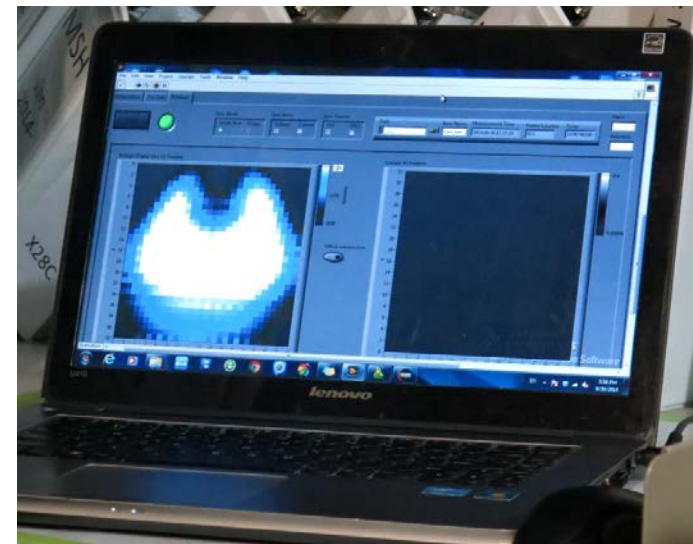
Detector Image



Torodial Mirror Focusing



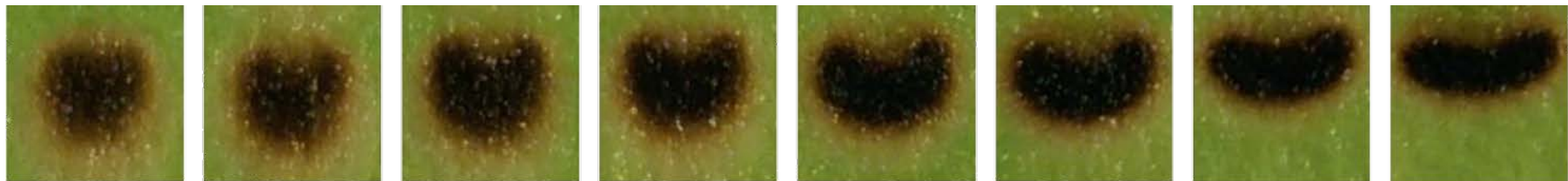
CHESS G3 Beam



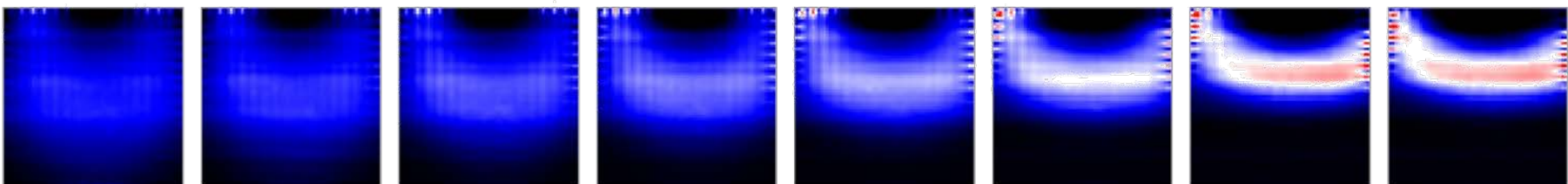
NSLS X28C Beam

Beam Imaging

X-ray Burn



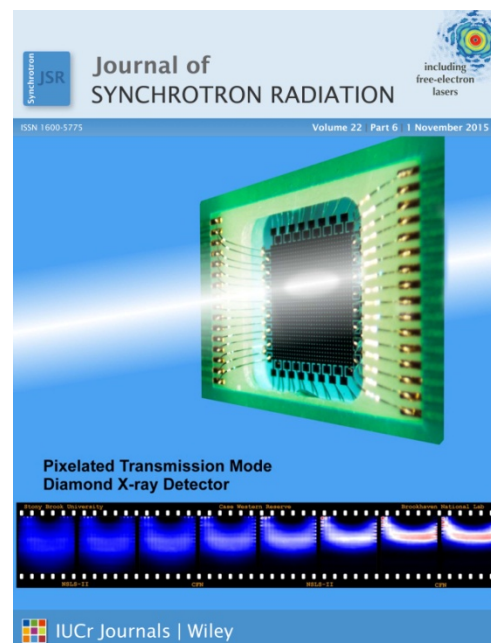
Detector Image



Torodial Mirror Focusing



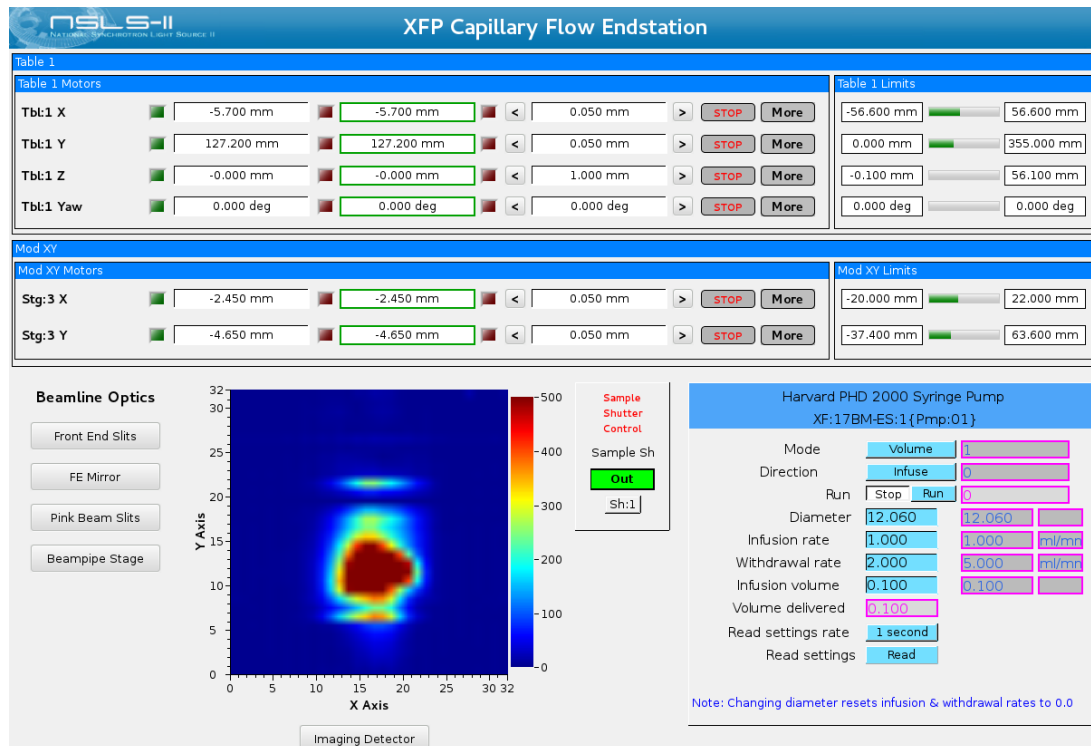
R&D100 2016 Finalist



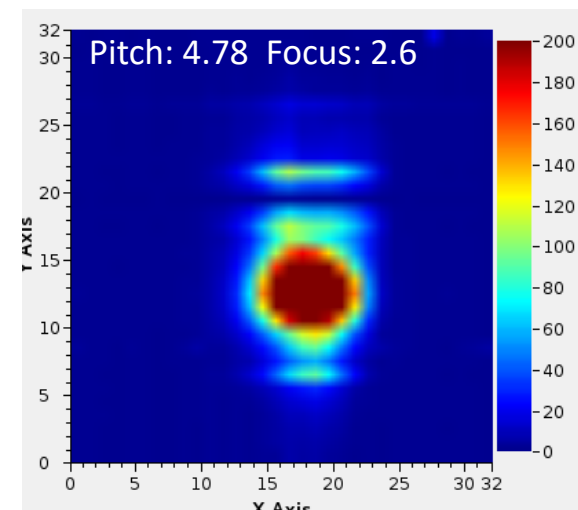
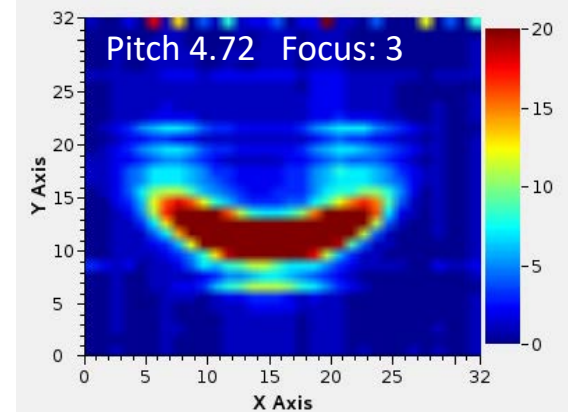
Zhou et al. (2015) JSR 22 :1396 (cover article)

Imaging Detector at NSLS-II XFP

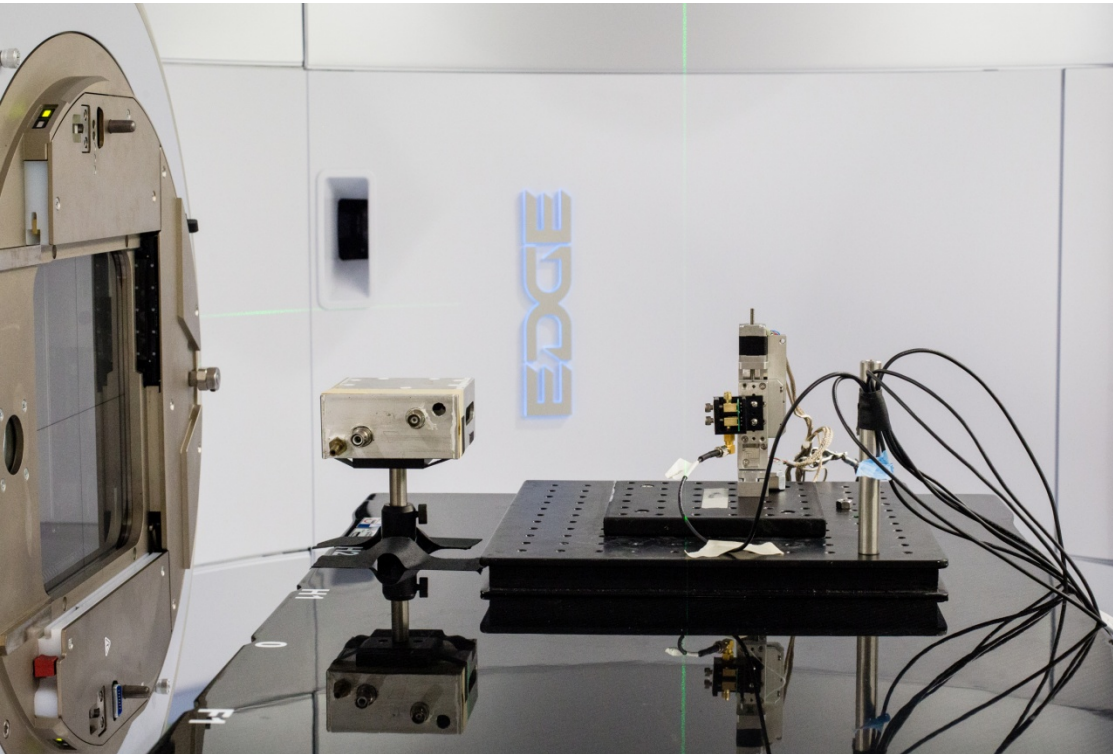
- Integrated into XFP Beamlne Controls System (EPICS/CSS)
- Used to align XFP toroidal focusing mirror (beamline commissioning)



Beam Images at Different Mirror Settings

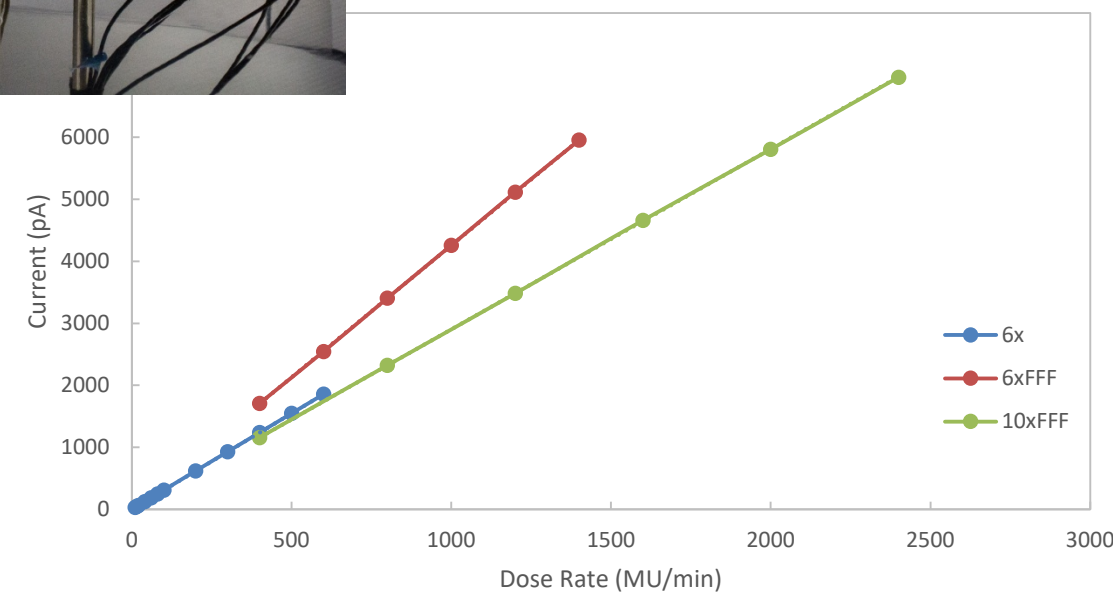


Gamma Ray Therapy



Diamond Detector Linearity

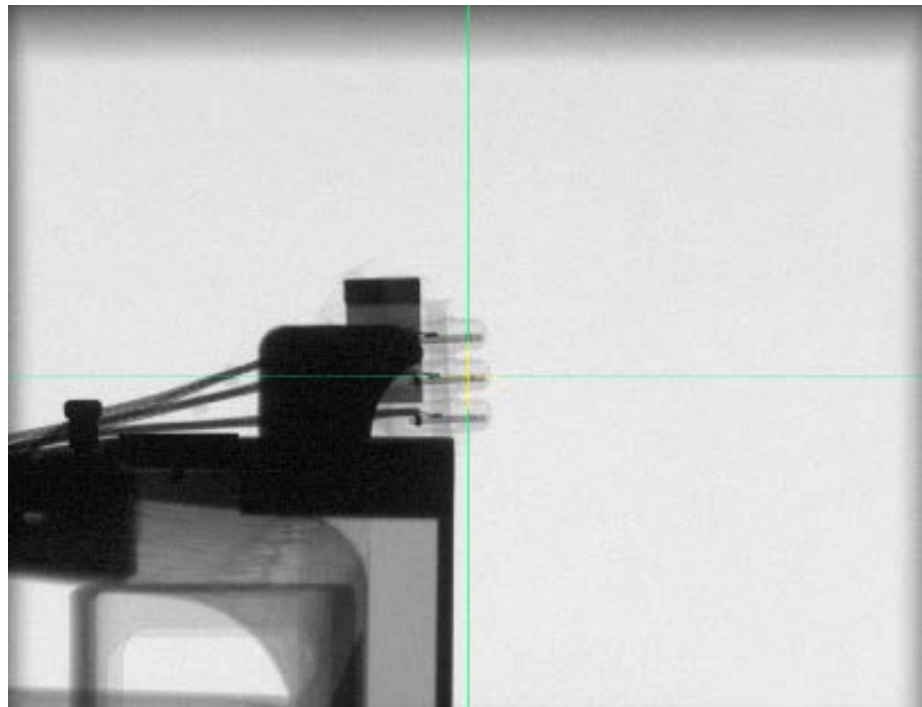
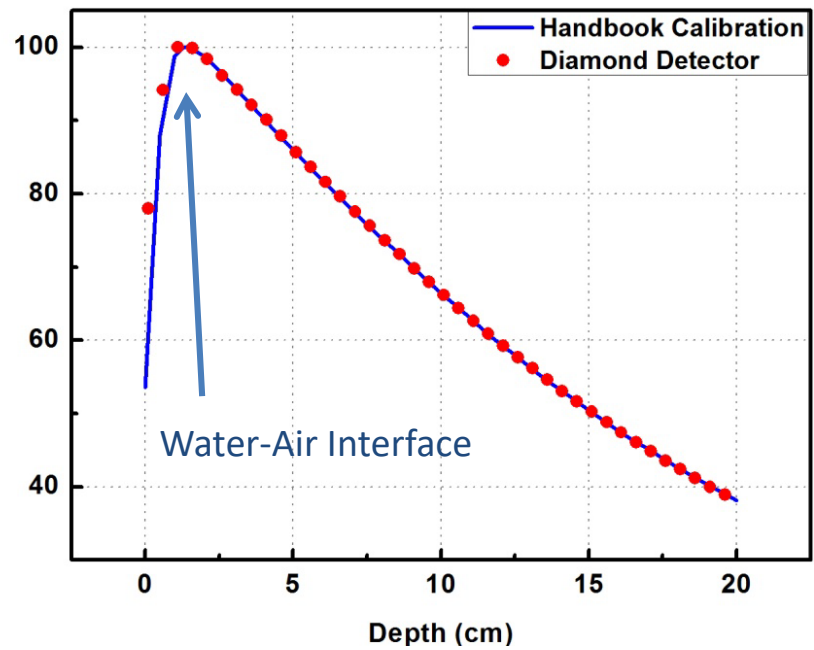
50 μm diamond shows less variation than “standard” ion chambers for machine calibration. Will also improve characterization of radiation field profile used for treatment.



Stony Brook
University

Intensity vs. Depth

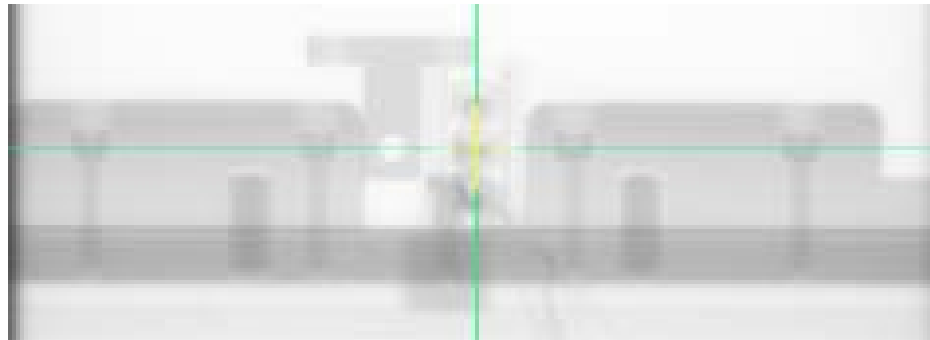
Normalized Intensity



$$I = I_o \cdot e^{-\mu \cdot d} \xrightarrow{\text{water}} I_o \cdot e^{-\mu \cdot \rho t}$$

- t (cm) is depth of water
- ρ (g/cm³) is density of water;

The mass absorption coefficient μ can be fitted as $0.0372 \text{ cm}^2/\text{g}$ in water
=> Gamma ray energy is ~3.5MeV

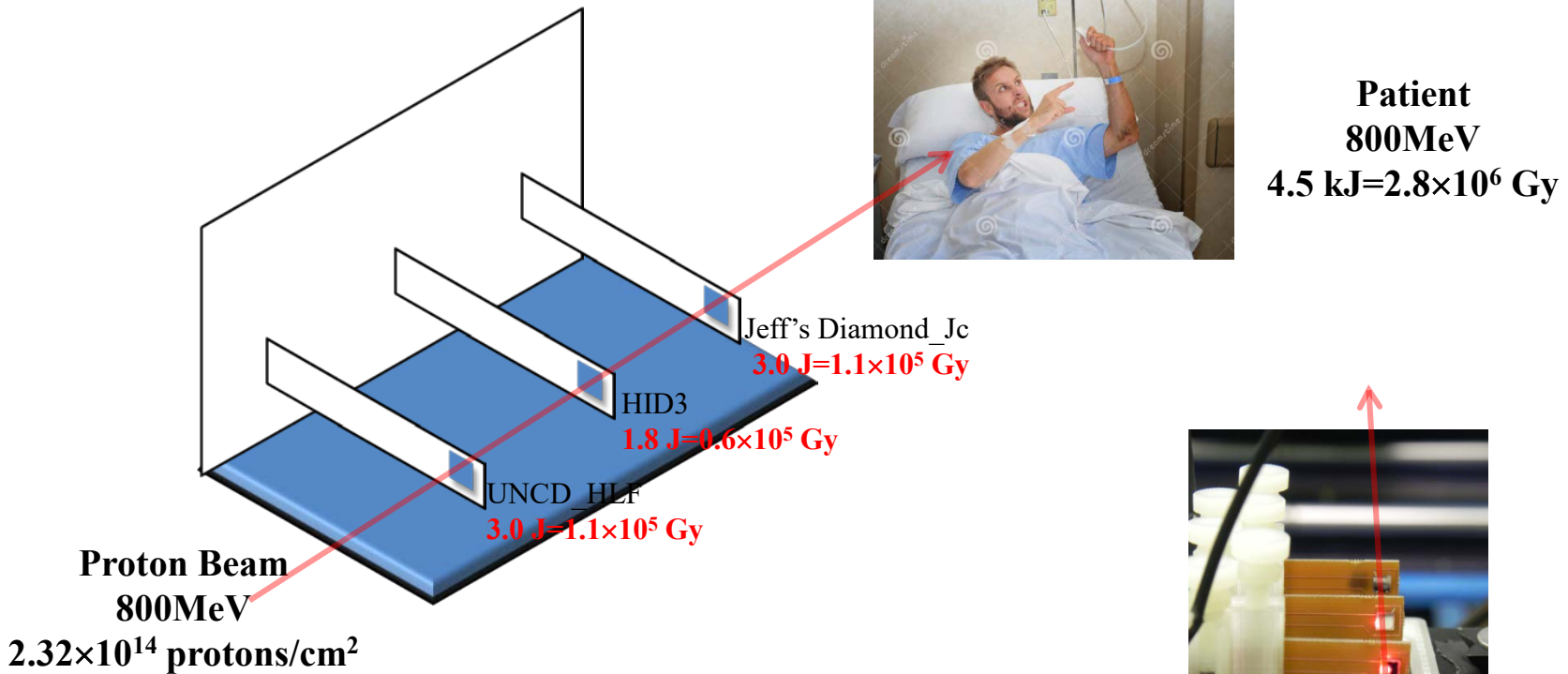


Proton Therapy – Radiation Damage

In principle, detector operation for protons is no different than for x-rays

Main difference – protons have sufficient momentum to damage the diamond lattice

=> Need to quantify radiation damage!



- Diamond Detector Power Absorption: 0.067%

- 10-years dose for medical use:

$$10 \text{ yrs} \times 350 \text{ days/yr} \times 8 \text{ hrs/day} \times 3 \text{ patients/hr} \times 2 \text{ shift/patient} \times (1 \sim 2 \text{ Gys}) = (1.68 \sim 3.36) \times 10^5 \text{ Gy}$$

- Corresponding diamond detector absorption radiation for 10-years medical dose:

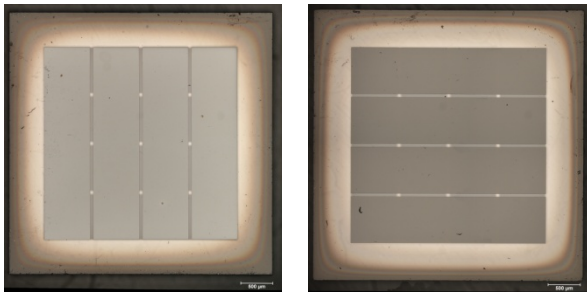
$$(1.68 \sim 3.36) \times 10^5 \text{ Gy} \times 0.067\% = (6.34 \sim 12.68) \times 10^3 \text{ Gy}$$

=> Delivered Dose is 100 yrs of normal operation!

LANL Radiation Set-up

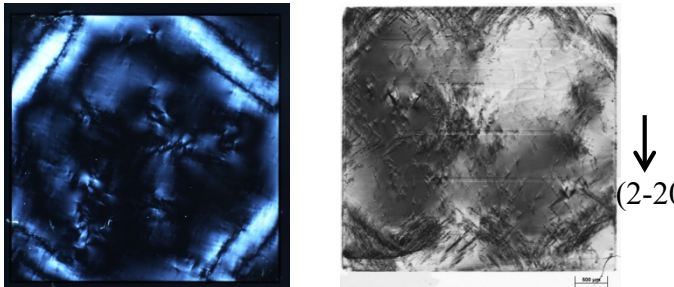
Proton Therapy – Radiation Damage

Optical Images



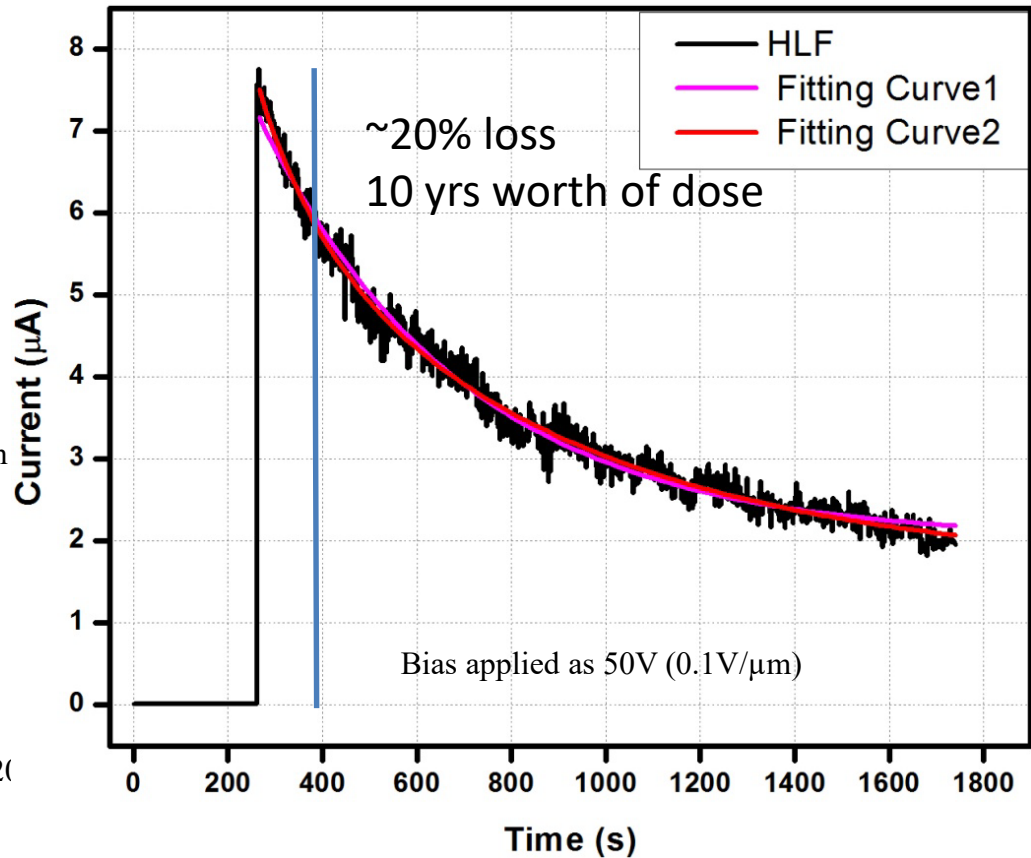
- Diamond thickness: $\sim 500\mu\text{m}$;
- Diamond Size: $4.11\text{mm} \times 4.10\text{mm}$;
- Active Area: $2.95\text{mm} \times 2.95\text{mm}$;
- Pattern Size: strip width=0.7mm; street=50 μm

Birefringence & Topography Image



- Birefringence image displays some slip band at corners;
- Topography displays low density dislocations in the active area;

During Proton Radiation

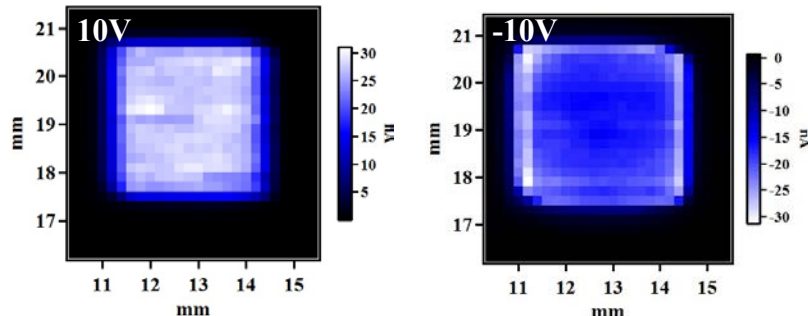


Radiation does not cause visible change, nor large scale structural change

However, the charge collection in the material does change, likely due to new trap centers

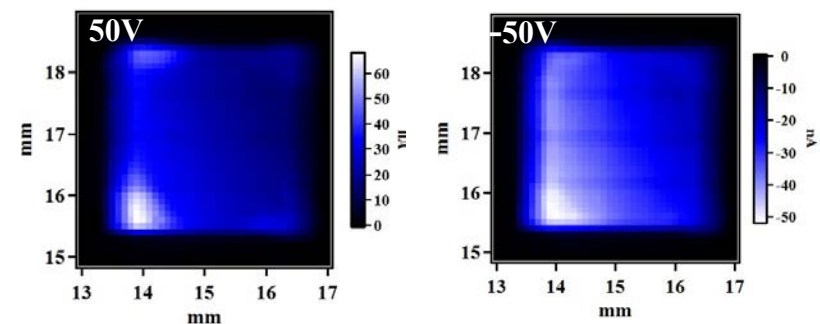
XBIC evaluation before and after Protons

Performance Before Radiation @CHESS G2

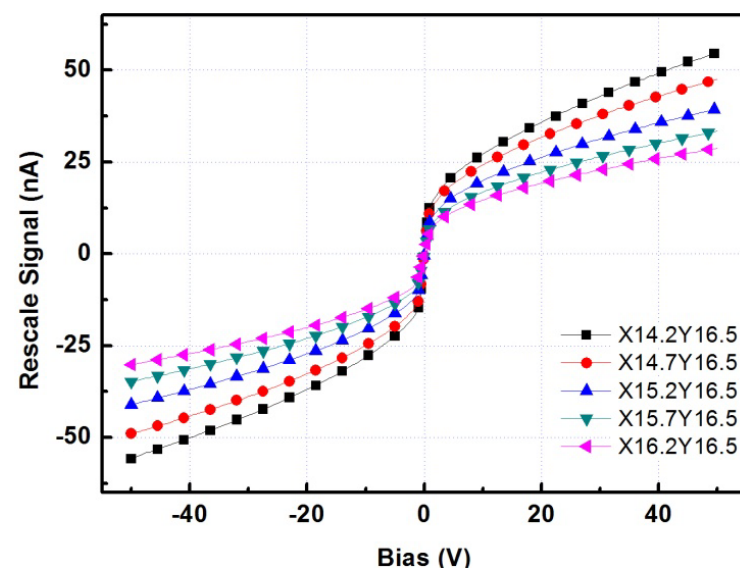
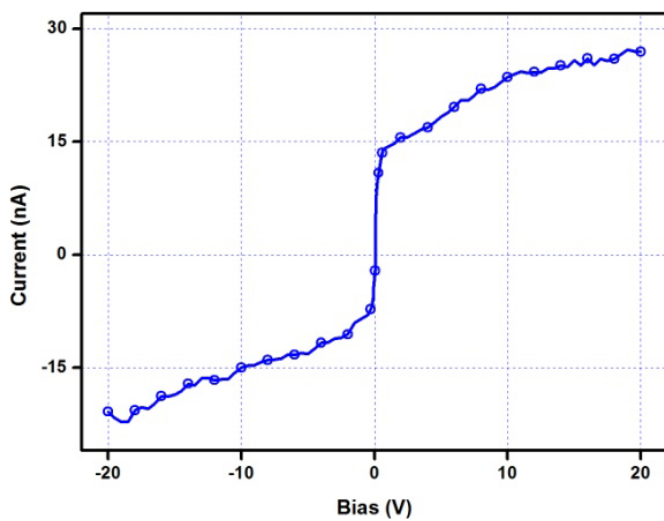


Initially uniform, even at low bias

Performance After Radiation @CHESS G2



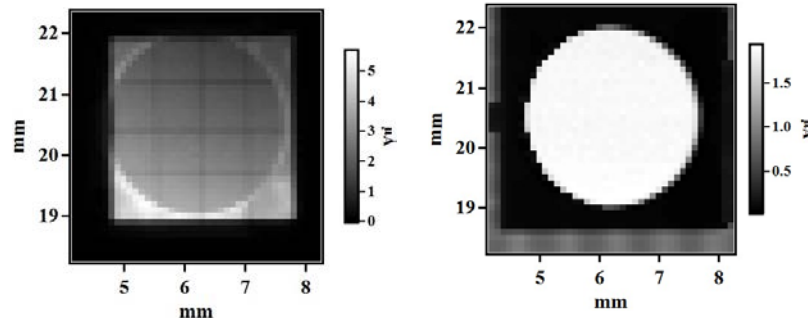
Proton beam gradient imprinted in device response post irradiation



Post irradiation, still unsaturated at 50V
22% to 45% of full collection

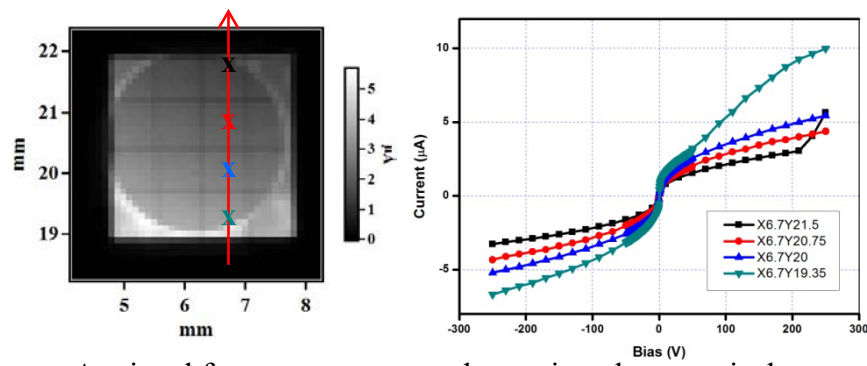
More performance tests after radiation @XFP (NSLS-II)

➤ Response Map @50V



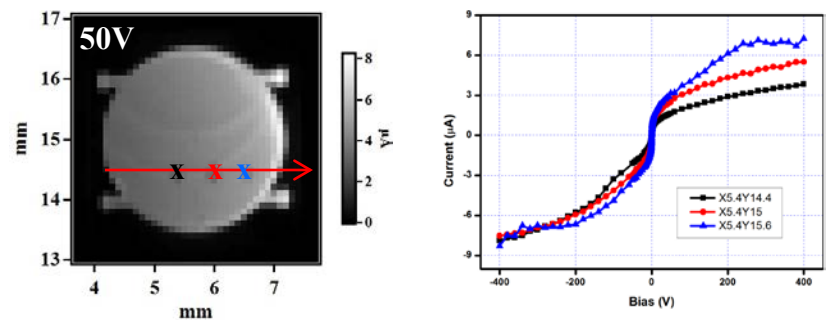
- Response map from monitor displays good uniformity
⇒ The varying signals in detector is from detector itself;
- From monitor's signal ($\sim 1.87\mu A$), detector's saturate signal should be $\sim 11.7\mu A$ (*actual signal is 1.6-4.7 μA*) ;
⇒ The decay ratio is 13.7%-40.2%.

➤ Bias Scan (Along vertical direction)



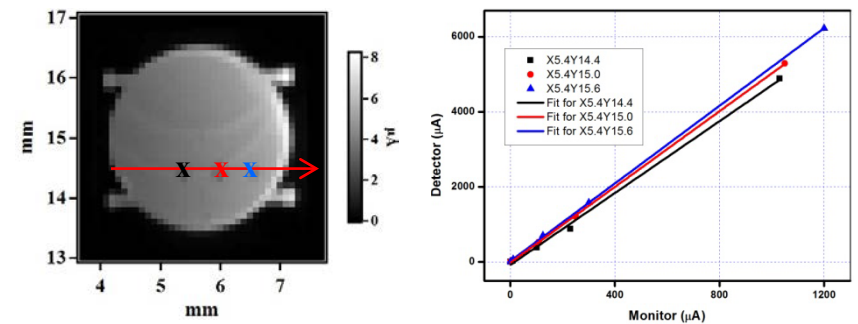
- As signal from response map decreasing along vertical direction, bias scan curve flattens in the same direction.

➤ Bias Scan (Along gradient direction)



- Bias scan curves are asymmetric under positive and negative bias;
- Signals under positive bias reflects gradient radiation on diamond;
- Detector's saturate signal should be $\sim 11.6\mu A$
⇒ The decay ratio is 25.9%-48.3%

➤ Flux Calibration (Along gradient direction)



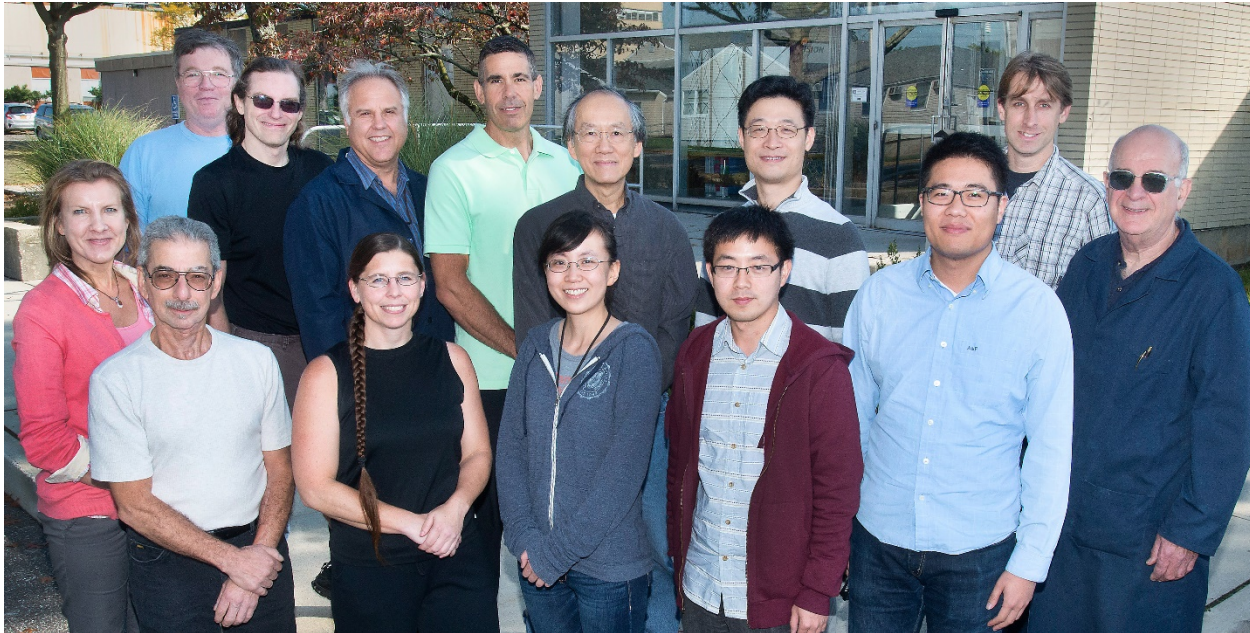
- Flux and response remain linear relationship, but the slopes change slightly according to radiation damage;

Conclusions

- Flux linearity demonstrated over ***11 orders of magnitude***
- X-ray BPMs monitors for monochromatic and white beam
- Commercialized by Sydor Instruments
 - 30+ devices at NSLS-II
 - Devices delivered to Diamond, APS, CHESS
- Position resolution of better than 50nm, and single bunch flux and position have been achieved
- 1k pixel transparent beam imager developed
- Proton and C-Ion imagers being tested
 - Radiation damage is observable but likely acceptable
 - Devices maintain flux linearity but lose spatial uniformity
 - Source is trapping sites within material, not gross structural changes

Thank you!

Acknowledgements



Stony Brook: Erik Muller, Tianyi Zhou, Mengnan Zou, Owen Ding, Sam Ryu, James Han, Jinkoo Kim

Instrumentation Division: John Smedley, Mengjia Gaowei, Gianluigi De Geronimo, Don Pinelli, John Triolo, Ron Angona, Howard Hansen, Albert Lum, Kim Ackley, John Walsh

Los Alamos: James Distel, Zhehui Wang, Ron Nelson

Case Western Reserve: Jen Bohon, Don Abel

CFN: Ming Lu

Bold = Diamond Group

NSLS-II: Elaine Di Masi, Klaus Attenkofer, Eli Stavitski

Cornell/CHESS: Arthur Woll, Howard Joress, Jacob Ruff

Applied Diamond: Joe Tabeling